20985

NATIONAL LIBRARY
OTTAWA

CANADA

BIBLIOTHÈQUE NATIONALE
OTTAWA

NAME OF AUTHOR... Igor CHOBOT

TITLE OF THESIS... TUBULAR MOTOR

UNIVERSITY... U of A, Edmonton

DEGREE FOR WHICH THESIS WAS PRESENTED... M. Sc.

YEAR THIS DEGREE GRANTED... Spring 1974

Permission is hereby granted to THE NATIONAL LIBRARY OF CANADA to microfilm this thesis and to lend or sell copies of the film.

The author reserves other publication rights, and neither the thesis nor extensive extracts from it may be printed or otherwise reproduced without the author's written permission.

(Signed)... Igor Chobot

PERMANENT ADDRESS:

5204 - 109 St

Edmonton

Alta

DATED... Jan. 28, 1974

NL-91 (10-68)

THE UNIVERSITY OF ALBERTA

TUBULAR MOTOR

BY

© IGOR CHOBOT

A THESIS

SUBMITTED TO THE FACULTY OF GRADUATE STUDIES AND

RESEARCH IN PARTIAL FULFILMENT OF THE REQUIREMENTS FOR

THE DEGREE OF MASTER OF SCIENCE

DEPARTMENT OF ELECTRICAL ENGINEERING

EDMONTON, ALBERTA

SPRING 1974

THE UNIVERSITY OF ALBERTA

FACULTY OF GRADUATE STUDIES AND RESEARCH

The undersigned certify that they have read, and recommend to the Faculty of Graduate Studies and Research for acceptance, a thesis entitled Tubular Motor submitted by Igor Chobot in partial fulfilment of the requirements for the degree of Master of Science.

J. K. Kelly
Supervisor

W. S. Neilson

R. H. King

Date Jan. 5, 1974

ABSTRACT

A field theory approach is used to develop the volt-ampere and force equations of an infinitely long tubular motor for quasi-static conditions. A circuit model is developed which includes the spatial harmonics of the electromagnetic fields.

Analysis of the effect of stator winding distribution, air gap width, rotor sleeve thickness and constant clearance shows that the air gap width should be as small as possible and the rotor sleeve thickness should be chosen to give optimum resistances for the best machine performance.

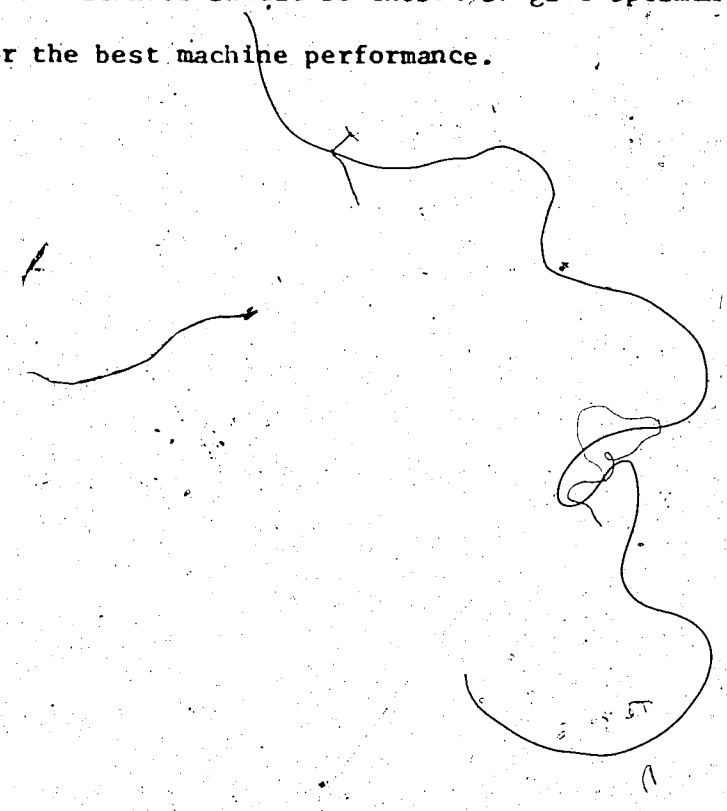

ACKNOWLEDGEMENTS

The author wishes to express his deep appreciation to Dr. D. H. Kelly for his guidance and supervision of this study.

The author also wishes to thank Mrs. E. Bell for her excellent typing of the thesis.

TABLE OF CONTENTS

TABLE OF CONTENTS (cont'd)

LIST OF FIGURES

LIST OF FIGURES (cont'd)

NOMENCLATURE

A	Fourier coefficient
a	subscript - relating to phase a
$\bar{A}$	magnetic vector potential
b	Fourier coefficient
b	subscript - relating to phase b
$\bar{B}$	magnetic flux density
d	subscript - relating to direct axis
$\bar{E}$	electric field intensity
F_e	electromagnetic force on rotor
$\bar{H}$	magnetic field intensity
i	instantaneous current
$\bar{I}$	current phasor
$\underline{I}$	current vector
J	current density
K, K', K''	constants
K_a^s	winding distribution factor
ℓ	length
L	inductance
N	number of conductors

NOMENCLATURE (cont'd)

p	d/dt
P	number of pole pairs
q	subscript - relating to quadrature axis
r	subscript - relating to rotor
R	resistance
s	subscript - relating to stator
s	slip
t	superscript - transpose
t	time variable
v	instantaneous voltage
$\bar{V}$	voltage phasor
$\underline{V}$	voltage vector
w_s	width of slot
W	stored energy
x, y, z	cartesian co-ordinate variables
X	reactance
Z	impedance

NOMENCLATURE (cont'd)

α	transformation matrix
λ	coefficient $2\pi\nu/\tau_r$
ν	order of spatial harmonic
ρ	resistivity
σ	conductivity
τ_r	length of repeatable section of stator
Φ	scalar potential
ω	angular frequency of supply
∇	curl operator
Im	imaginary part
Re	real part
*	superscript - complex conjugate

CHAPTER I

INTRODUCTION

1.1. Linear Induction Machine

Extensive pioneering work on linear induction motors was done by Laithwaite (2) about a decade ago. Today many engineers are involved in projects on transit systems, using single-sided and double-sided linear machines as a means of propulsion.

A linear induction motor can be simply described as a conventional rotary machine (Fig. 1-1) which has been cut along an axial plane and opened out flat (Fig. 1-2) to give a single-sided linear induction motor (LIM). Addition of a second stator (Fig. 1-3) leads to a double-sided LIM. Considering relative rotor and stator lengths, LIMs may be divided into two classes. These classes have been termed as short-stator (rotor longer than stator) and short-rotor (stator longer than rotor) machines.

If the model in Fig. 1-2 is re-rolled about an axis parallel to the direction of the field motion, the resulting model (Fig. 1-4a) represents the basic structure of a tubular motor. The winding of the tubular motor consists of an array of coils (Fig. 1-4b), having no end turns.

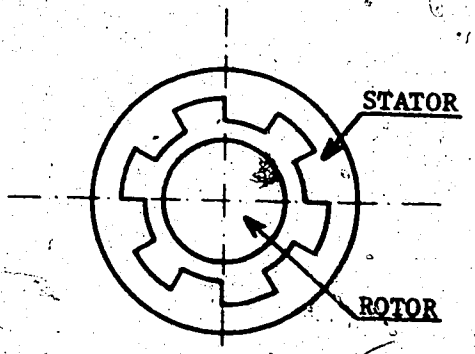

FIG. 1-1 CONVENTIONAL INDUCTION MACHINE

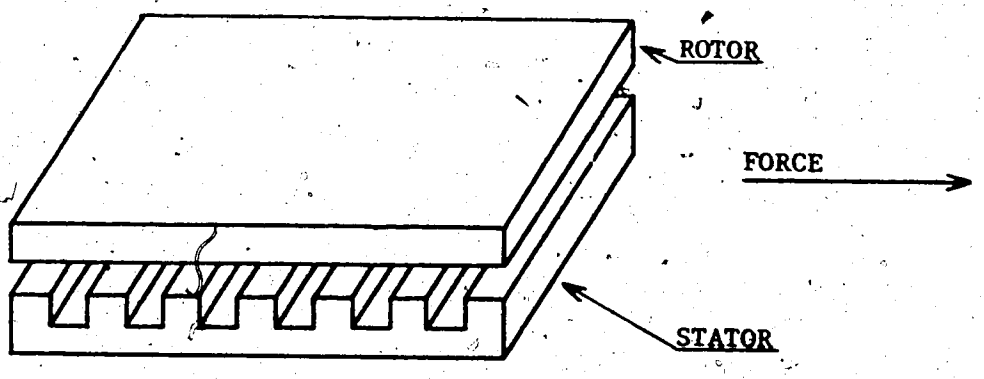

FIG. 1-2 SINGLE-SIDED LIM

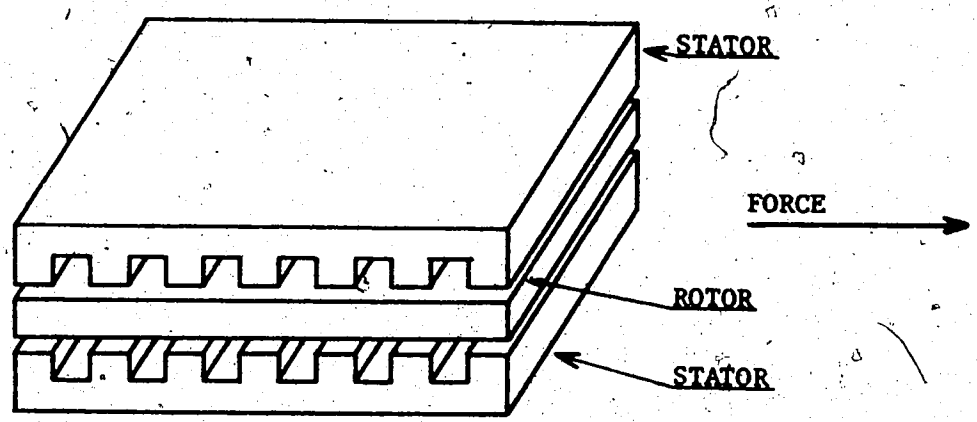

FIG. 1-3 DOUBLE-SIDED LIM

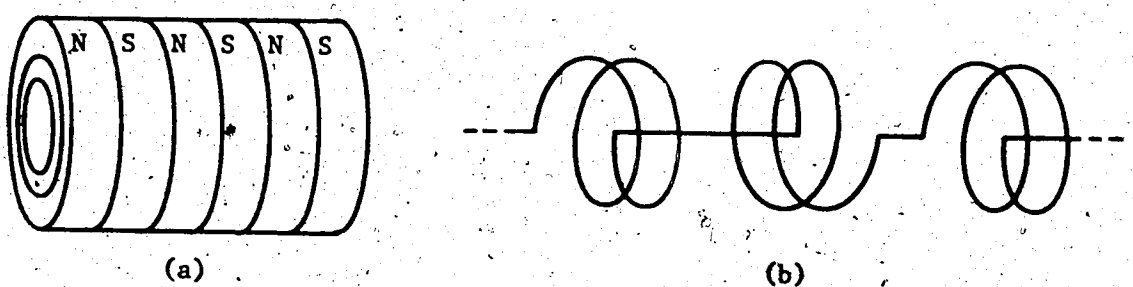

FIG. 1-4 TUBULAR MOTOR

(a) basic structure
(b) array of coils

As can be seen from Fig. 1-4a, where N and S represent alternate N and S poles, the tubular motor is an axial-flux machine. The flux is forced axially along the rotor, therefore the rotor must contain iron if the magnetic circuit is to be at all reasonable.

A number of liquid metal induction pumps employing the use of tubular stator windings have been devised for pumping liquid bismuth, sodium or potassium. Utilizing the same winding arrangements and replacing the liquid metal with a copper or aluminium sleeve may result in two different methods of constructing the rotor. In general, the rotor sleeve may be permanently affixed to the rotor iron or the rotor iron may be held by some external means while the rotor sleeve is allowed to glide (6). The analysis in the following chapters is applicable for both types of rotor structure.

1.2. Method of Analysis

The classical analysis of induction machines (11) applied to the tubular motor would not be adequate because of considerations such as large air gaps and lack of definitive rotor conductors. Therefore, a field theory approach (such as used by (1,3)) is necessary and is used to develop the force expressions for steady state sinusoidal excitation.

Energy conversion characteristics of a polyphase induction machine with symmetrical impedances can be derived from an equivalent two-phase induction machine by a change of variables (5). For this reason a two-phase tubular motor is considered for simplicity.

A lumped parameter circuit model based on the field theory is developed as the circuit model offers advantages in the computation of

input and output quantities under steady state conditions.

Tubular motors operate at low frequencies (usually 50 or 60 Hz), therefore a quasi-static approach (1,3,5) is used to determine the fields in the air gap. Equivalent inductances of the machine are found from the magnetic storage energy and then the equations of motion are derived. Using linear axis transformations, the spatial dependance of the rotor inductances is removed and an equivalent circuit is found. Spatial harmonics of the current densities are included, resulting in a model which consists of a set of harmonic machines with series-connected stator windings and a common output shaft.

Calculations of the forces are done on a digital computer and are compared for different values of air gap, stator winding distribution and rotor conductivity.

1.3. Objective of Thesis

The steady-state characteristics of a tubular motor are derived from equations of motion based on the field theory. An APL program is set up to calculate steady state force, efficiency, input current and harmonic forces for different values of rotor slip. The effect of the rotor sleeve thickness, air gap thickness and stator winding distribution on the machine performance is examined. This is done for two kinds of rotor sleeve material - copper and aluminum.

CHAPTER II

ELECTROMAGNETIC FIELD

Electromagnetic field equations are developed from Maxwell's equations for a described model. In essence, the field equations are partial differential equations. These are solved subject to the given boundary conditions.

2.1. Assumptions

The following simplifying assumptions will be made in deriving the field equations:

(a) The stator and rotor iron cores are laminated so that conductivity (σ) is zero. They have a permeability μ for which $\mu >> \mu_o$ holds and therefore μ is assumed to be infinitely large.

(b) The tubular motor (Fig. 2-1) is replaced by the model shown in Fig. 2-2, and the coordinate system is as shown. This model is adequate if the air gap is small with respect to the rotor diameter.

(c) The longitudinal effect of the motor is neglected (both the rotor and stator are infinitely long in the z direction).

(d) The air gap is uniform.

(e) For the operating frequency of 60 Hz the current density of both the rotor and stator is uniform in the z direction, that is, the skin effect is neglected.

(f) The stator conductors are not skewed.

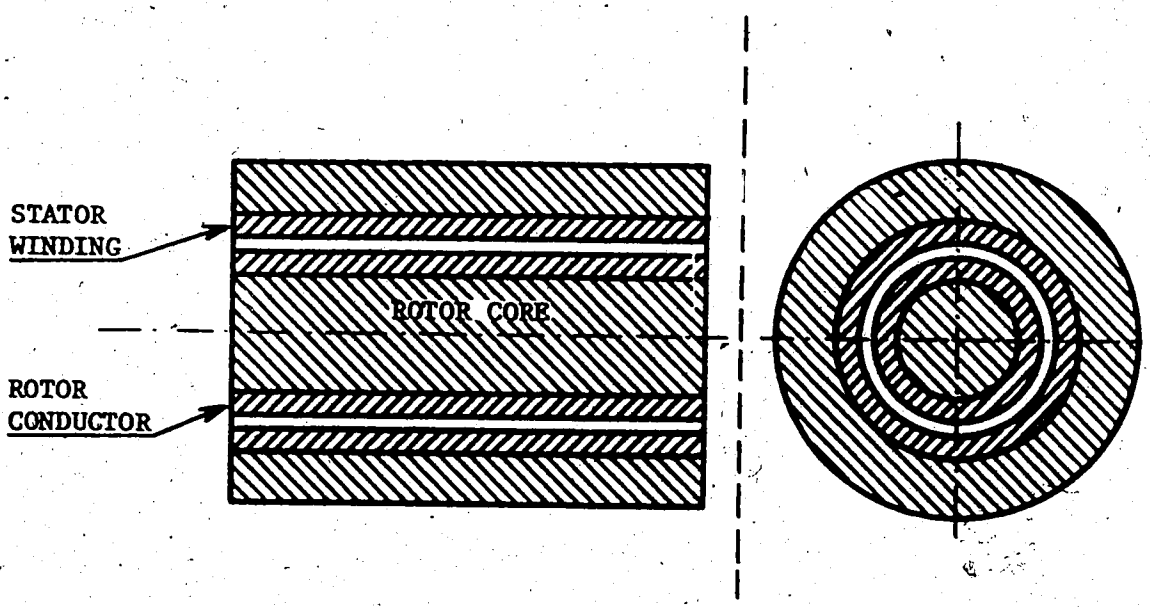

FIG. 2-1 TUBULAR MACHINE

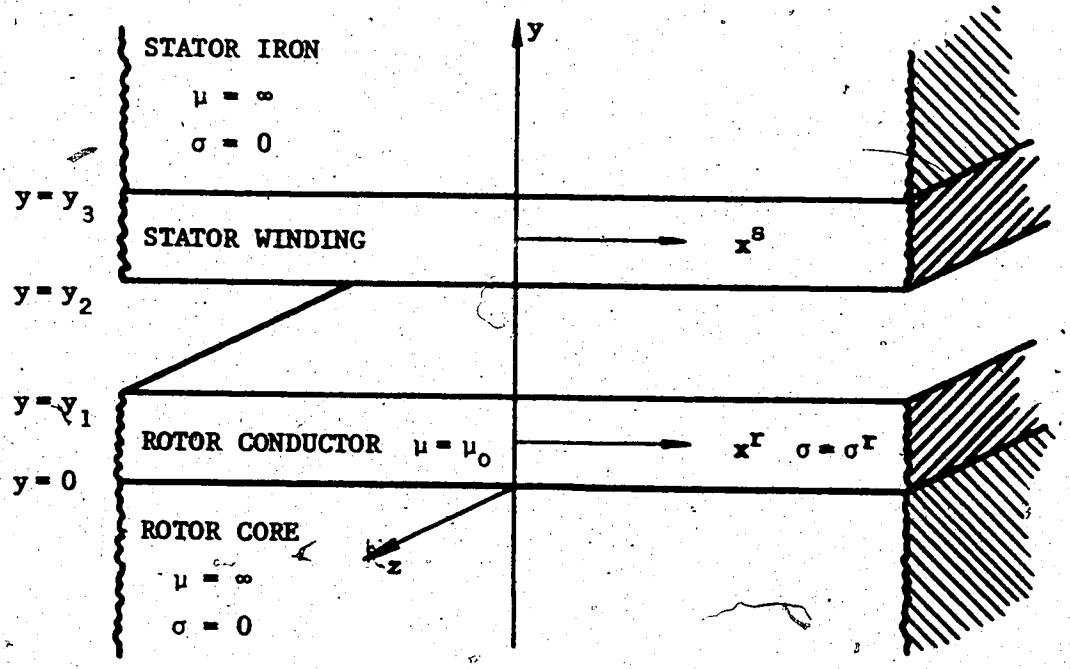

FIG. 2-2 CARTESIAN CO-ORDINATE SYSTEM

2.2. Stator and Rotor Current Densities

Three different types of stator windings are considered. The type I winding (14) as shown in Fig. 2-3 is the simplest and least expensive winding to make. The type II and III windings produce the current density distribution as shown in Fig. 2-5 and Fig. 2-6 respectively.

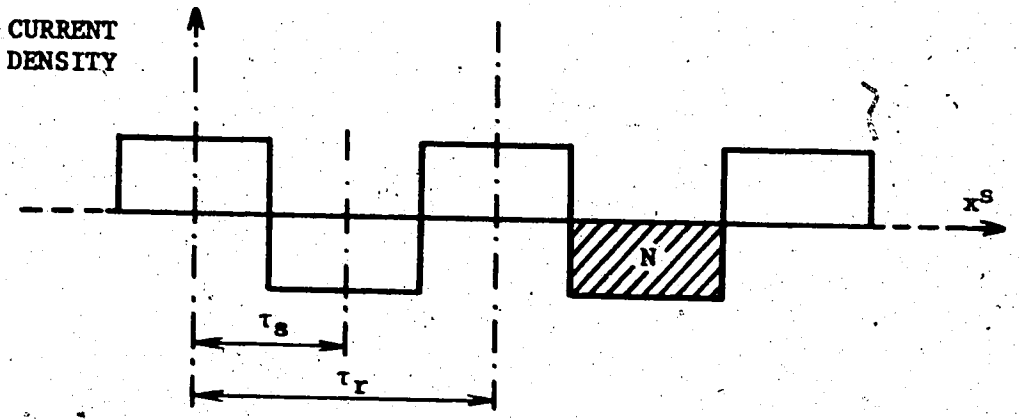

FIG. 2-3 STATOR WINDING (one phase) TYPE I

The stator winding is not replaced by a current sheet, thus the winding has a finite thickness which is represented by the value of $|y_3 - y_2|$ in Fig. 2-2. In general, the stator current density will be of the form as shown in Fig. 2-4.

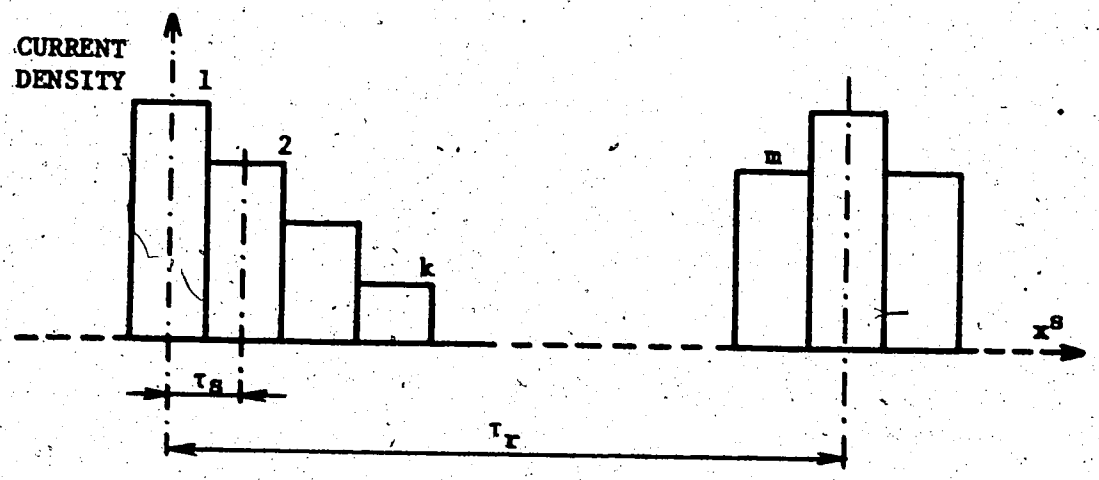

FIG. 2-4 GENERAL STATOR CURRENT DENSITY (one phase)

Following the method introduced by Hague and developed by Saunders (3) and Nasar (4), the stator current density is defined as

$$J'_{zj} = \frac{N_j\, i_j}{w_s\,(y_3 - y_2)} \quad \text{(amperes/meter}^2\text{)} \qquad (2\text{-}1)$$

The k^{th} stator current density pulse (Fig. 2-4) is generally expressed in the Fourier series

$$h_k(x) = \frac{N_k\, i}{w_s\, w_r} \sum_{\nu=1}^{\infty} (a_{k\nu} \cos \lambda_\nu x + b_\nu \sin \lambda_\nu x)$$

where

$$\lambda_\nu = \frac{2\pi\nu}{\tau_r} \qquad w_r = y_3 - y_2$$

and

$$a_{k\nu} = \frac{2}{\tau_r} \int_{\frac{\tau_r}{2}}^{\tau_r/2} f(x) \cos \lambda_\nu x \, dx$$

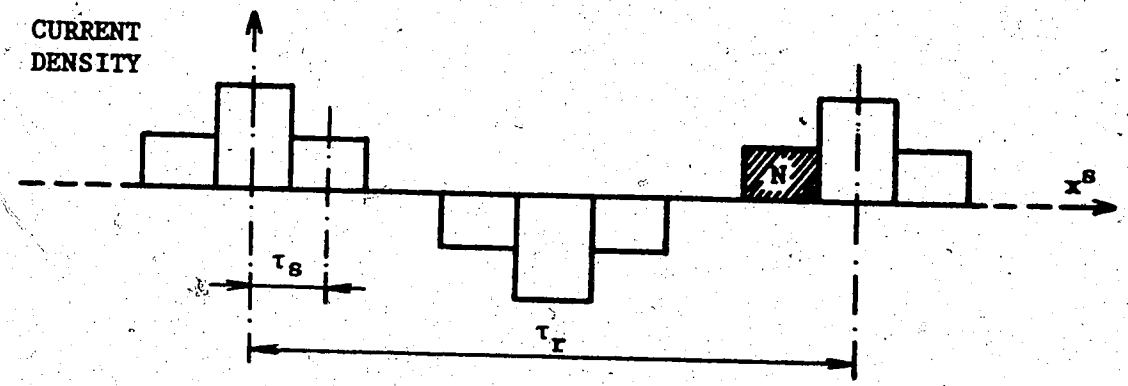

FIG. 2-5 STATOR WINDING (one phase) TYPE II

Substituting for f (x) and for the limits, we have

$$a_{k\nu} = \frac{2}{\tau_r \lambda_\nu} \left[\sin\lambda_\nu (x_o + w_s) - \sin\lambda_\nu x_o\right]$$

Similarly,

$$b_{k\nu} = \frac{2}{\lambda_\nu \tau_r} \left[\cos\lambda_\nu x_o - \cos\lambda_\nu (x_o + w_s)\right]$$

The overall current density sheet consists of m pulses separated from each other by τ_s. Then

$$h(x) = \sum_{k=1}^{m} h_r(x) = \sum_{k=1}^{m} \frac{N_k i}{w_s w_r} \sum_{\nu=1}^{\infty} (a_{k\nu} \cos\lambda_\nu x + b_\nu \sin\lambda_\nu x) \qquad (2\text{-}2)$$

Assuming that the stator conductors are distributed symmetrically about the centre line of phase A as shown in Fig. 2-4

$$b_\nu{}^s = \sum_{k=1}^{m} \frac{b_{k\nu} N_k i_b{}^s}{w_s w_r} \quad \text{and} \quad a_\nu{}^s = \sum_{k=1}^{m} \frac{a_{k\nu} N_k i_a{}^s}{w_s w_r}$$

Choosing the origin such that $x_o = -\frac{w_s}{2}$, then

$$a_\nu = \frac{2 i_a{}^s}{\tau_r} \frac{\sin (\lambda_\nu w_s/2)}{(w_r \lambda_\nu w_s/2)} \sum_{k=1}^{m} N_k \cos [\lambda_\nu (k-1)\tau_s] =$$

$$= \frac{K_{a\nu}}{y_3 - y_2} \; i_a{}^s \qquad (2\text{-}3)$$

Similarly, for phase B

$$b_\nu = \frac{2\, i_b^s}{\tau_r} \frac{\sin(\lambda_\nu w_s/2)}{(w_r \lambda_\nu w_s/2)} \sum_{k=1}^{m} N_k \sin[\lambda_\nu (k-1)\tau_s] =$$

$$= \frac{K_{b\nu}}{y_3 - y_2}\, i_b^s \qquad (2\text{-}4)$$

and $K_{a\nu} = K_{b\nu}$, due to the symmetry of the winding.

Rotor currents are restricted to the rotor sleeve, the rotor core being laminated. In general, the rotor current densities are

$$J_{za}{}^r = \sum_{\nu=i}^{\infty} a_\nu{}^r \cos\lambda_\nu x^r \qquad \text{(amperes/meter}^2\text{)}$$

$$J_{zb}{}^r = \sum_{\nu=i}^{\infty} b_\nu{}^r \sin\lambda_\nu x^r \qquad \text{(amperes/meter}^2\text{)} \qquad (2\text{-}5)$$

and

$$J_z{}^r = \sum_{\nu=1}^{\infty} a_\nu{}^r \cos\lambda_\nu x^r + b_\nu{}^r \sin\lambda_\nu x^r \qquad (2\text{-}6)$$

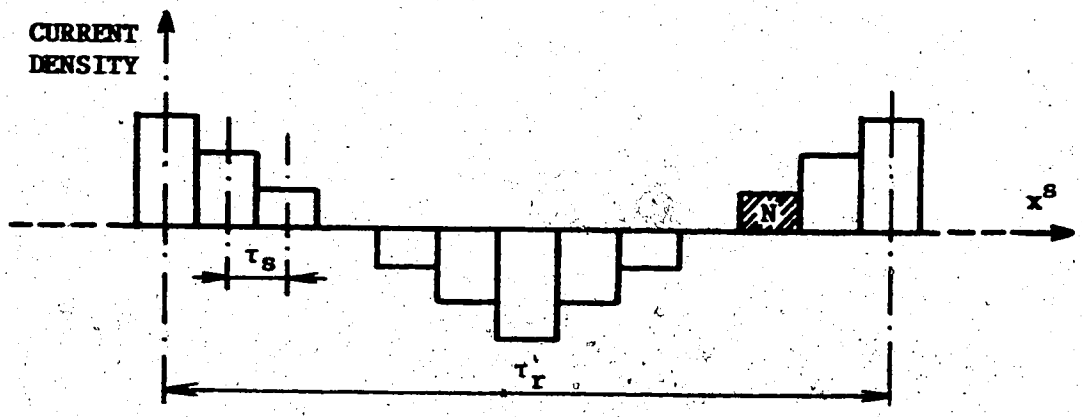

FIG. 2-6 STATOR WINDING (one phase) TYPE III

2.3. Field Equations

Electromagnetic fields in the stator winding, air gap and the rotor sleeve are derived from Maxwell's equations

$$\nabla \cdot \bar{B} = 0 \tag{2-7}$$

$$\nabla \cdot \bar{D} = \rho \tag{2-8}$$

$$\nabla \times \bar{H} = \bar{J} + \frac{\partial}{\partial t} \epsilon \bar{E} \tag{2-9}$$

$$\nabla \times \bar{E} = - \frac{\partial \bar{B}}{\partial t} \tag{2-10}$$

$$\bar{J} = \sigma \bar{E} \tag{2-11}$$

$$\bar{B} = \mu \bar{H} \tag{2-12}$$

It is advantageous to use both the vector potential $\bar{A}$ and scalar potential ϕ.

We have

$$\nabla \times \bar{E} + \frac{\partial \bar{B}}{\partial t} = 0 \tag{2-13}$$

and $\nabla \cdot \bar{B} = 0$

Since the divergence of the curl of any vector vanishes, we can satisfy the above by setting

$$\bar{B} = \nabla \times \bar{A} \tag{2-14}$$

Then

$$\nabla \times \bar{E} + \frac{\partial \bar{B}}{\partial t} = \frac{\partial}{\partial t} (\nabla \times \bar{A}) + \nabla \times \bar{E} = \nabla \times (\frac{\partial \bar{A}}{\partial t} + \bar{E}) = 0 \tag{2-15}$$

Since the curl of the gradient of any function vanishes, the above can be satisfied by setting

$$\bar{E} + \frac{\partial \bar{A}}{\partial t} = - \nabla \Phi \qquad (2\text{-}16)$$

therefore

$$\bar{E} = - \frac{\partial \bar{A}}{\partial t} - \nabla \Phi \qquad (2\text{-}17)$$

Substituting (2-14) and (2-17) into (2-9) gives

$$\varepsilon \frac{\partial}{\partial t} \left(- \frac{\partial \bar{A}}{\partial t} - \nabla \Phi\right) = \mu \nabla \times \bar{B} - \bar{J}$$

or $$\mu\varepsilon \frac{\partial}{\partial t} \left(- \frac{\partial \bar{A}}{\partial t} - \nabla \Phi\right) = \mu \nabla \times \bar{H} - \mu \bar{J} \qquad (2\text{-}18)$$

To simplify the above, the Lorentz condition

$$\nabla \cdot \bar{A} + \mu\varepsilon \frac{\partial \Phi}{\partial t} = 0$$

is imposed, then

$$\nabla^2 \bar{A} - \mu\varepsilon \frac{\partial^2 \bar{A}}{\partial t^2} = - \mu \bar{J} \qquad (2\text{-}19)$$

For quasi-static conditions, displacement current is negligible and equations (2-19) become

$$\nabla^2 \bar{A} = - \mu \bar{J} \qquad (2\text{-}20)$$

In the quasi-static system the energy that can be attributed to the electromagnetic fields is stored in the magnetic field (18). Magnetic stored energy in the machine is

$$W_m = \frac{1}{2} \int_{\text{volume}} \bar{B} \cdot \bar{H} \, dv \qquad (2\text{-}21)$$

The stator currents are z-directed so that rotor currents are also z-directed. Equations 2-20 become

$$\nabla^2 \bar{A}_z = -\mu \bar{J}_z^s \quad \text{in the stator conductor} \qquad (2\text{-}22)$$

$$-\mu \bar{J}_z^r \quad \text{in the rotor conductor} \qquad (2\text{-}23)$$

$$\text{and} \quad 0 \quad \text{elsewhere} \qquad (2\text{-}24)$$

If $\bar{A}_z$ is expressed as a series

$$A_z = \sum_{\nu=1}^{\infty} A_{z\nu} \qquad (2\text{-}25)$$

Each component of the series can be found independently due to the linearity of the system, therefore

$$\nabla^2 A_z = \nabla^2 \sum_{\nu=1}^{\infty} A_{z\nu} = \sum_{\nu=1}^{\infty} \nabla^2 A_{z\nu} \qquad (2\text{-}26)$$

The tubular motor has three regions to be considered (Fig. 2-2)

(1) the stator conductor $y_3 \geq y \geq y_2$
(2) the air gap $y_2 \geq y \geq y_1$
(3) the rotor conductor $y_1 \geq y \geq 0$

Laplace s equation is solved in Appendix A in detail. The following expressions are the field equations of the machine.

(i) Stator conductor

$$H_x = \lambda_\nu[(K_1 \sinh\lambda_\nu y + K_3 \cosh\lambda_\nu y) \cos\lambda_\nu + \\ + (K_2 \sinh\lambda_\nu y + K_4 \cosh\lambda_\nu y) \sin\lambda_\nu x] \qquad (2\text{-}27)$$

$$B_y = \mu\lambda_\nu[(K_1 \cosh\lambda_\nu y + K_3 \sinh\lambda_\nu y) \sinh\lambda_\nu x - \\ - (K_2 \cosh\lambda_\nu y + K_4 \sinh\lambda_\nu y) \cos\lambda_\nu x + \\ + \frac{1}{\lambda_\nu^2}(a^s \sin\lambda_\nu x - b^s \cos\lambda_\nu x)] \qquad (2\text{-}28)$$

(ii) Air gap

$$H_x = \lambda_\nu[(K_1' \sinh\lambda_\nu y + K_3' \cosh\lambda_\nu y) \cos\lambda_\nu x + \\ + (K_2' \sinh\lambda_\nu y + K_4' \cosh\lambda_\nu y) \sin\lambda_\nu x] \qquad (2\text{-}29)$$

$$B_y = \mu\lambda_\nu[(K_1' \cosh\lambda_\nu y + K_3' \sinh\lambda_\nu y) \sin\lambda_\nu x - \\ - (K_2' \cosh\lambda_\nu y + K_4' \sinh\lambda_\nu y) \cos\lambda_\nu x] \qquad (2\text{-}30)$$

(iii) Rotor conductor

$$H_x = \lambda_\nu[(K_1'' \sinh\lambda_\nu y + K_3'' \cosh\lambda_\nu y) \cos\lambda_\nu x + \\ + (K_2'' \sinh\lambda_\nu y + K_4'' \cosh\lambda_\nu y) \sin\lambda_\nu x] \qquad (2\text{-}31)$$

$$B_y = \mu\lambda_\nu [(K_1'' \cosh\lambda_\nu y + K_3'' \sinh\lambda_\nu y) \sin\lambda_\nu x -$$

$$- (K_2'' \cosh\lambda_\nu y + K_4'' \sinh\lambda_\nu y) \cos\lambda_\nu x +$$

$$+ \frac{1}{\lambda_\nu^2} (C_1 \sin\lambda_\nu x - C_2 \cos\lambda_\nu x)] \qquad (2\text{-}32)$$

in which

$$C_1 = (a_\nu{}^r \sin\lambda_\nu x_o{}^r + b_\nu{}^r \cos\lambda_\nu x_o{}^r)$$

$$C_2 = (a_\nu{}^r \cos\lambda_\nu x_o{}^r - b_\nu{}^r \sin\lambda_\nu x_o{}^r) \qquad (2\text{-}33)$$

In equations (2-27) to (2-33) subscript ν is omitted for convenience for the constants K (i.e. K_1 is $K_{1\nu}$).

2.4. Boundary Conditions

For the given model we have to consider two different interfaces: conductor air and conductor iron. We can use the same general approach (Fig. 2-7), the result of which has to be modified for the conductor iron interface.

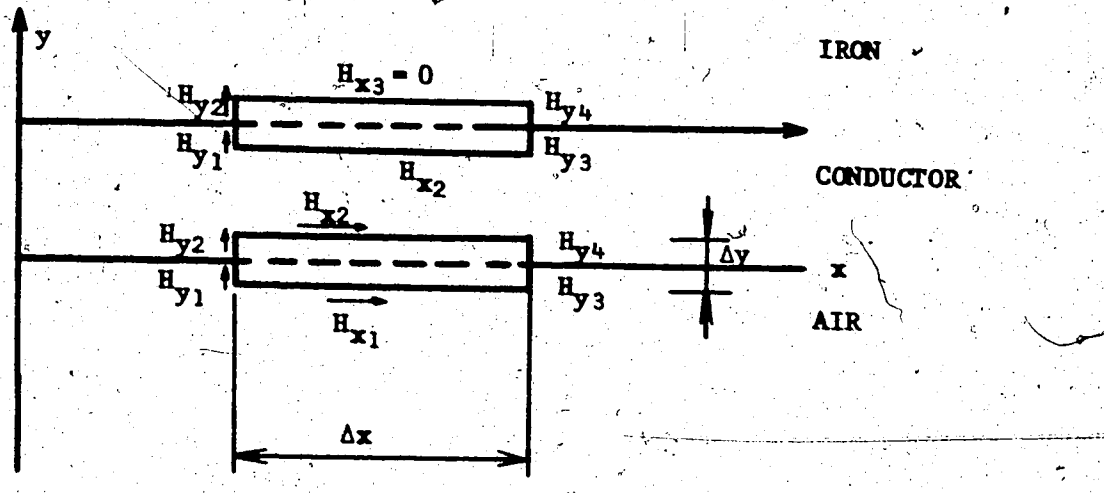

FIG. 2-7 BOUNDARY CONDITIONS

Applying Maxwell's equations, we have

$$\oint \bar{H} \cdot ds = \int (\dot{\bar{D}} + \bar{J}) \cdot d\bar{a}$$

which becomes

$$H_{x_1} \Delta x + H_{y_3} \frac{\Delta y}{2} + H_{y_4} \frac{\Delta y}{2} - H_{x_2} \Delta x - H_{y_2} \frac{\Delta y}{2} - H_{y_1} \frac{\Delta y}{2} = J_z \Delta x \Delta y$$

If the current density is considered to be finite, then as $\Delta y \to 0$ we have

$$H_{x_1} \Delta x - H_{x_2} \Delta x = 0$$

or $H_{x_1} = H_{x_2}$, continuous

for the conductor-air interface.

For the conductor-iron interface, $H_{x\,iron} = 0$, therefore $H_{x_2} = H_{x_3} = 0$.

It can be shown (16) that the other boundary conditions are $B_{y_1} = B_{y_2}$ for the conductor-air interface and $B_{y_2} = B_{y_3}$ for the conductor-iron interface.

Applying the boundary conditions to the field equations, the K coefficients are evaluated as follows:

(i) For $y = 0$, $H_x = 0$

$$H_x = \lambda[(K_1'' \sinh\lambda y + K_3'' \cosh \lambda y) \cos\lambda x +$$

$$+ (K_2'' \sinh\lambda y + K_4'' \cosh\lambda y) \sin\lambda x] = 0$$

gives

$$K_3'' \cos\lambda x + K_4'' \sin\lambda x = 0$$

which is satisfied for

$$K_3'' = K_4'' = 0 \tag{2-34}$$

(ii) H_x and B_y continuous, $y = y_1$

Equating (2-31) and (2-29)

$$\begin{aligned}(K_1'' - K_1') \sinh\lambda y_1 &= K_3' \cosh\lambda y_1 \\ (K_2'' - K_2') \sinh\lambda y_1 &= K_4' \cosh\lambda y_1\end{aligned} \tag{2-35}$$

B_y is continuous, therefore

$$\begin{aligned}(K_1'' - K_1') \cosh\lambda y_1 - K_3' \sinh\lambda y_1 + \frac{C_1}{\lambda^2} &= 0 \\ (K_2'' - K_2') \cosh y_1 - K_4' \sinh y_1 + \frac{C_2}{\lambda^2} &= 0\end{aligned} \tag{2-36}$$

(iii) $y = y_2$

H_x and B_y continuous

$$\begin{aligned}(K_1 - K_1') \sinh\lambda y_2 + (K_3 - K_3') \cosh\lambda y_2 &= 0 \\ (K_2 - K_2') \sinh\lambda y_2 + (K_4 - K_4') \cosh\lambda y_2 &= 0 \\ (K_1' - K_1) \cosh\lambda y_2 + (K_3' - K_3) \sinh\lambda y_2 - \frac{a^s}{\lambda^2} &= 0 \\ (K_2' - K_2) \cosh y_2 + (K_4' - K_4) \sinh\lambda y_2 - \frac{b^s}{\lambda^2} &= 0\end{aligned} \tag{2-37}$$

(iv) $y = y_3,\ H_x = 0$

$$K_1 \sinh\lambda y_3 + K_3 \cosh\lambda y_3 = 0$$

$$K_2 \sinh\lambda y_3 + K_4 \cosh\lambda y_3 = 0 \qquad (2\text{-}38)$$

From equations (2-34) to (2-38) we have

$$K_1 = \frac{C_1}{\lambda^2} \sinh\lambda y_1 \coth\lambda y_3 - \frac{a^s}{\lambda^2} \sinh\lambda y_2 \coth\lambda y_3$$

$$K_2 = \frac{C_2}{\lambda^2} \sinh\lambda y_1 \coth\lambda y_3 - \frac{b^s}{\lambda^2} \sinh\lambda y_2 \coth\lambda y_3$$

$$K_3 = K_3' + \frac{a^s}{\lambda^2} \sinh\lambda y_2$$

$$K_4 = K_4' + \frac{b^s}{\lambda^2} \sinh\lambda y_2$$

$$K_1' = K_1 + \frac{a^s}{\lambda^2} \cosh\lambda y_2$$

$$K_2' = K_2 + \frac{b^s}{\lambda^2} \cosh\lambda y_2$$

$$K_3' = -\frac{C_1}{\lambda^2} \sinh\lambda y_1$$

$$K_4' = -\frac{C_2}{\lambda^2} \sinh\lambda y_1$$

$$K_1'' = K_1 + \frac{a^s}{\lambda^2} \cosh\lambda y_2 - \frac{C_1}{\lambda^2} \cosh\lambda y_1$$

$$K_2'' = K_2 + \frac{b^s}{\lambda^2} \cosh\lambda y_2 - \frac{C_2}{\lambda^2} \cosh\lambda y_1$$

$$K_3'' = 0$$

$$K_4'' = 0 \qquad (2\text{-}39)$$

The set of equations (2-39) lists the K coefficients for the field equations (2-27) to (2-33).

CHAPTER III

EQUIVALENT MACHINE PARAMETERS

The parameters of the machine must be found in order to determine the equations of motion. First, equivalent inductances of the machine are evaluated from the energies stored in electric and magnetic fields.

3.1. Magnetic Stored Energy

Energy stored in electric fields (4) is

$$W_e = \frac{1}{2} \int_v \bar{D} \cdot \bar{E} \, dv$$

Under quasi-static conditions this is negligible.

Energy stored in magnetic fields is given by (2-21)

$$W_m = \frac{1}{2} \int_v \bar{B} \cdot \bar{H} \, dv$$

or $$W_m = \frac{1}{2\mu} \int_v |B|^2 \, dv = \frac{1}{2\mu} \int_0^{y_3} \int_0^{\ell} \int_0^{\frac{P\tau_r}{2}} (B_x^2 + B_y^2) \, dv \qquad (3\text{-}1)$$

and $$W_m = W_1 + W_2 + W_3 \qquad (3\text{-}2)$$

where W_1, W_2 and W_3 are the energies stored within the stator winding, air gap and the rotor winding respectively.

The details of the calculations are given in Appendix B. Equation (3-2) becomes

$$W_m = \frac{\ell\mu P\pi}{4} \sum_{\nu=1}^{\infty} \nu \left\{ \left[\frac{a_\nu r^2 + b_\nu r^2}{\lambda_\nu^4} \right] [\sinh^2\lambda_\nu y_1 \coth\lambda_\nu y_3 + \right.$$

$$+ \lambda_\nu y_1 - \sinh\lambda_\nu y_1 \cosh\lambda_\nu y_1] +$$

$$+ \left[\frac{a_\nu s^2 + b_\nu s^2}{\lambda_\nu^4} \right] [\sinh^2\lambda_\nu y_2 \coth\lambda_\nu y_3 + \lambda_\nu (y_3 - y_2) -$$

$$- \sinh\lambda_\nu y_2 \cosh\lambda_\nu y_2] + \frac{2}{\lambda_\nu^4} [(a_\nu^s a_\nu^r + b_\nu^s b_\nu^r) \cos\lambda_\nu x_o^r +$$

$$+ (b_\nu^s a_\nu^r - a_\nu^s b_\nu^r) \sin\lambda_\nu x_o^r] \cdot$$

$$\left. \cdot [\sinh\lambda_\nu y_1 \cosh\lambda_\nu y_2 - \sinh\lambda_\nu y_1 \sinh\lambda_\nu y_2 \coth\lambda_\nu y_3] \right\}$$

(3-3)

Representing the hyperbolic functions by the first two terms of the corresponding series and dropping the fifth and higher order terms of λ_ν, we have

$$W_m = \frac{\ell\mu P\pi}{8y_3} \sum_{\nu=1}^{\infty} \frac{1}{\lambda_\nu^2} \{ [a_\nu s^2 + b_\nu s^2] (y_3 - y_2)^2 [1 + \lambda_\nu^2 \frac{y_2^2}{3}] +$$

$$+ 2 [(a_\nu^s a_\nu^r + b_\nu^s b_\nu^r) \cos\lambda_\nu x_o^r + (b_\nu^s a_\nu^r -$$

$$- a_\nu^s b_\nu^s) \sinh\lambda_\nu x_o^r] y_1 (y_3 - y_2) [1 + \frac{\lambda_\nu^2}{6} (y_1^2 +$$

$$+ y_2^2 - 2\, y_2\, y_3)] + [a_\nu r^2 + b_\nu r^2]\; y_1^2 \left[1 + \lambda_\nu^2 \frac{(y_3 - y_1)^2}{3}\right]\}$$

(3-4)

The magnetic stored energy in the above equation is a function of several variables among which are rotor conductor, air gap and stator conductor thickness.

3.2. Inductances and Resistances

The actual machine is replaced by a coupled system having two windings at right angles (1, 5) on the phase axes. The rotor and stator windings carry currents i_a^r, i_b^r, i_a^s and i_b^s respectively, the subscripts referring to the winding (phase a, phase b) and the superscripts referring to the coil set (stator - s, and rotor - r). The magnetic stored energy is then

$$W_m = \frac{1}{2} \int_\nu \bar{H} \cdot \bar{B}\, dv = \frac{1}{2} \sum_{i=1}^{n} \sum_{j=1}^{m} L_{ij}\, i_i\, i_j =$$

$$= \sum_{\nu=1}^{\infty} \frac{1}{2} \left[\sum_{i=1}^{n} \sum_{j=1}^{m} L_{ij}\, i_i\, i_j\right] =$$

$$= \sum_{\nu=1}^{\infty} \frac{1}{2} [L_{aa\nu}^{ss} (i_{a\nu}^s)^2 + L_{ab\nu}^{ss} (i_{a\nu}^s\, i_{b\nu}^s) +$$

$$+ L_{ba\nu}^{ss} (i_{b\nu}^s\, i_{a\nu}^s) + L_{bb\nu}^{ss} (i_{b\nu}^s)^2 + L_{aa\nu}^{rr} (i_{a\nu}^r)^2 +$$

$$+ L_{ab\nu}^{rr} (i_{a\nu}{}^{r} i_{b\nu}{}^{r}) + L_{ba\nu}^{rr} (i_{b\nu}{}^{r} i_{a\nu}{}^{r}) + L_{bb\nu}^{rr} (i_{b\nu}{}^{r})^{2} +$$

$$+ L_{aa\nu}^{sr} (i_{a\nu}{}^{s} i_{a\nu}{}^{r}) + L_{aa\nu}^{rs} (i_{a\nu}{}^{r} i_{a\nu}{}^{s}) + L_{ab\nu}^{sr} (i_{a\nu}{}^{s} i_{b\nu}{}^{r}) +$$

$$+ L_{ba\nu}^{rs} (i_{b\nu}{}^{r} i_{a\nu}{}^{s}) + L_{ba\nu}^{sr} (i_{b\nu}{}^{s} i_{a\nu}{}^{r}) + L_{ab\nu}^{rs} (i_{a\nu}{}^{r} i_{b\nu}{}^{s}) +$$

$$+ L_{bb\nu}^{sr} (i_{b\nu}{}^{s} i_{b\nu}{}^{r}) + L_{bb\nu}^{rs} (i_{b\nu}{}^{r} i_{b\nu}{}^{s})] \qquad (3\text{-}5)$$

where L^{ss} and L^{rr} are the self-inductances and L^{sr} and L^{rs} are the mutual inductances.

Relating currents in (3-5) to the actual current densities, the inductances are determined by equating (3-5) and (3-4).

The rotor coil is assumed to have the same distribution and number of turns as the stator winding (1).

$$K_{a\nu}{}^{s} i_{a\nu}{}^{r} \cos \lambda_{\nu} x^{r} = y_{1} a_{\nu}{}^{r} \cos \lambda_{\nu} x^{r} \qquad (3\text{-}6)$$

which gives

$$a_{\nu}{}^{r} = \frac{K_{a\nu}{}^{s}}{y_{1}} i_{a\nu}{}^{r}$$

$$b_{\nu}{}^{r} = \frac{K_{a\nu}{}^{s}}{y_{1}} i_{a\nu}{}^{r} \qquad (3\text{-}7)$$

Rewriting (2-3) and (2-4) for the stator current densities

$$a_\nu^s = \frac{K_{a\nu}^s}{y_3 - y_2} i_a^s$$

$$b_\nu^s = \frac{K_{a\nu}^s}{y_3 - y_2} i_b^s \qquad (3\text{-}8)$$

Using (3-7) and (3-8), the inductances of the equivalent machine are determined by equating (3-4) and (3-5). Then

$$L_{ab\nu}^{ss} = L_{ba\nu}^{ss} = L_{ab\nu}^{rr} = L_{ba\nu}^{rr} = 0$$

$$L_{aa\nu}^{sr} = L_{aa\nu}^{rs} = L_{bb\nu}^{sr} = L_{bb\nu}^{rs} = L_{sr\nu} \cos \lambda_\nu x_o^r$$

$$L_{ab\nu}^{sr} = L_{ba\nu}^{rs} = - L_{ba\nu}^{sr} = - L_{ab\nu}^{rs} = - L_{sr\nu} \sin \lambda_\nu x_o^r$$

$$L_{aa\nu}^{ss} = L_{bb\nu}^{ss} = L_{ss\nu}$$

$$L_{aa\nu}^{rr} = L_{bb\nu}^{rr} = L_{rr\nu}$$

$$L_{ss\nu} = \frac{P\ell\mu\tau(K_{a\nu}^s)^2}{4\lambda_\nu^2 y_3} \left[1 + \lambda_\nu^2 \frac{y_2^2}{3} \right]$$

$$L_{rr\nu} = \frac{P\ell\mu\tau(K_{a\nu}^s)^2}{4\lambda_\nu^2 y_3} \left[1 + \lambda_\nu^2 \frac{(y_3 - y_1)^2}{3} \right]$$

$$L_{sr\nu} = \frac{P\ell\mu\tau(K_{a\nu}^s)^2}{4\lambda_\nu^2 y_3} \left[1 + \frac{\lambda_\nu^2}{6} (y_1^2 + y_2^2 - 2 y_2 y_3) \right] \qquad (3\text{-}9)$$

The resistances of both the stator windings are assumed equal, i.e.

$$R_a^s = R_b^s = R_{av}^s = R_{bv}^s = \frac{P}{2} \sum_{j=1}^{k} N_j \, R \text{ (of the conductor)} \tag{3-10}$$

and are associated with the first space harmonic (1), therefore

$$\begin{aligned} R_{av}^s = R_{bv}^s = R_a^s \quad & \text{for } v = 1 \\ = 0 \quad & \text{for } v \neq 1 \end{aligned} \tag{3-11}$$

The equivalent resistances of the rotor are found by equating rotor losses in the actual and equivalent machines. The total instantaneous rotor power dissipation in a machine is

$$P_d = \frac{\rho^r}{2} \int \int \int \left[J_x{}^{r2} + J_y{}^{r2} + J_z{}^{r2} \right] dx^r \, dy \, dz \tag{3-12}$$

which for our model becomes

$$P_d = \frac{\rho^r}{2} \, P \ell^r \int_0^{y_1} \int_0^{\tau_r} (J_a{}^{r2} + J_b{}^{r2}) \, dx^r \, dy \tag{3-13}$$

Integrating the above equation, the equivalent rotor resistances are

$$R_{av}{}^r = R_{bv}{}^r = \frac{P \ell^r \tau_r (K_{av}{}^s)^2}{4 \sigma^r y_1} \tag{3-14}$$

The equivalent inductances and resistances derived in this chapter are coil variables dependent upon the relative positions of the rotor and stator axes.

CHAPTER IV

DEVELOPMENT OF FORCE EQUATIONS

4.1. Equations of Motion

Equations of motion are best expressed in matrix notation, which is used throughout the chapter. As done in (1), it is convenient to subscript the matrix rather than the individual harmonic variables in the matrix.

The volt-amp equations are given by

$$\underline{V_{ab}} = \sum_{\nu=1}^{\infty} (\underline{R}_\nu + p\ \underline{L}_\nu)\ \underline{I}_{ab} \tag{4-1}$$

where

$$\underline{V}_{ab} = \begin{bmatrix} v_a^s \\ v_b^s \\ 0 \\ 0 \end{bmatrix} \qquad \underline{I}_{ab\nu} = \begin{bmatrix} i_{a\nu}^s \\ i_{b\nu}^s \\ i_{a\nu}^r \\ i_{b\nu}^r \end{bmatrix} = \begin{bmatrix} i_a^s \\ i_b^s \\ i_a^r \\ i_b^r \end{bmatrix}_\nu \tag{4-2}$$

$$\underline{R}_\nu = \begin{bmatrix} R_a^s & 0 & 0 & 0 \\ 0 & R_b^s & 0 & 0 \\ 0 & 0 & R_a^r & 0 \\ 0 & 0 & 0 & R_b^r \end{bmatrix}_\nu \tag{4-3}$$

and $$p = \frac{d}{dt}$$

We have

$$\underline{L}_\nu = \left[\begin{array}{cc|cc} L_{ss} & 0 & L_{sr}\cos\lambda x^r & -L_{sr}\sin\lambda x^r \\ 0 & L_{ss} & L_{sr}\sin\lambda x^r & L_{sr}\cos\lambda x^r \\ \hline L_{sr}\cos\lambda x^r & L_{sr}\sin\lambda x^r & L_{rr} & 0 \\ -L_{sr}\sin\lambda x^r & L_{sr}\cos\lambda x^r & 0 & L_{rr} \end{array}\right]_\nu \qquad (4\text{-}4)$$

The electromagnetic force on the rotor (1) is

$$F_e{}^r = \sum_{\nu=1}^{\infty} F_{e\nu}{}^r = \frac{1}{\partial x^r}\left[\partial W_m - \sum_{\nu=1}^{\infty} \sum_{\text{coils}} i_{j\nu}\, d\lambda_{j\nu}\right] \qquad (4\text{-}5)$$

Assuming a linear magnetic circuit

$$F_e{}^r = \sum_{\nu=1}^{\infty} \sum_{\text{coils}} i_{j\nu}\, \frac{\partial \lambda_{j\nu}}{\partial x^r} \qquad (4\text{-}6)$$

or $$F_{e\nu}{}^r = \frac{1}{2}\, \underline{I}^t_{ab\nu}\, \underline{F}^r_{ab\nu}\, \underline{I}_{ab\nu} \qquad (4\text{-}7)$$

where

$$\underline{I}^t_{ab\nu} = [i_a{}^s \;\; i_b{}^s \;\; i_a{}^r \;\; i_b{}^r]_\nu \qquad (4\text{-}8)$$

and

$$\underline{F}^{r}_{ab\nu} = \frac{\partial \underline{L}_{\nu}}{\partial x^{r}} = L_{sr\nu}\lambda_{\nu} \begin{bmatrix} 0 & 0 & -\sin\lambda x^{r} & -\cos\lambda x^{r} \\ 0 & 0 & \cos\lambda x^{r} & -\sin\lambda x^{r} \\ -\sin\lambda x^{r} & \cos\lambda x^{r} & 0 & 0 \\ -\cos\lambda x^{r} & -\sin\lambda x^{r} & 0 & 0 \end{bmatrix}_{\nu} \tag{4-9}$$

4.2. dq Transformation

Equations (4-1) and (4-7) describe the behaviour of the machine under all operating conditions, however, they are non-linear.

Applying a linear dq transformation, the space dependance of the equivalent inductances and resistances is removed. The transformation is power invariant (5) and is defined as

$$\underline{I}_{ab\nu} = \underline{\alpha}_{\nu}\, \underline{I}_{dq\nu} \tag{4-10}$$

and

$$\underline{V}_{ab\nu} = \underline{\alpha}_{\nu}\, \underline{V}_{dq\nu} \tag{4-11}$$

where

$$\underline{\alpha}_{\nu} = \begin{bmatrix} 1 & 0 & 0 & 0 \\ 0 & 1 & 0 & 0 \\ 0 & 0 & \cos\lambda x^{r} & \sin\lambda x^{r} \\ 0 & 0 & -\sin\lambda x^{r} & \cos\lambda x^{r} \end{bmatrix}_{\nu} \tag{4-12}$$

The following equation holds for the transformation matrix:

$$\underline{\alpha}_\nu^t = \underline{\alpha}_\nu^{-1} \tag{4-13}$$

Equation (4-10) implies that the set of rotor currents $i_{a\nu}^r$ and $i_{b\nu}^r$ in the rotor windings moving with the stator is transformed to the currents i_d^r and i_q^r which are stationary with respect to the stator reference frame. It means that the air gap fields produced by currents i_a^r and i_b^r are the same as the fields produced by the currents i_d^r and i_q^r flowing in the fictitious windings stationary to the stator.

We have

$$\underline{V}_{dq\nu} = \underline{\alpha}_\nu^t \; \underline{V}_{ab\nu} \tag{4-14}$$

Substituting (4-1) into (4-14)

$$\underline{V}_{dq\nu} = \sum_{\nu=1}^{\infty} \underline{\alpha}^t (\underline{R}_\nu + p \; \underline{L}_\nu) \underline{\alpha}_\nu \; \underline{I}_{dq\nu} =$$

$$= \sum_{\nu=1}^{\infty} (\underline{R}_{dq\nu} + \underline{L}_{dq\nu} \, p + \underline{E}_{dq\nu}^r \, \dot{x}^r) \underline{I}_{dq\nu} \tag{4-15}$$

where

$$\underline{R}_{dq\nu} = \underline{\alpha}^t \; \underline{R}_\nu \; \underline{\alpha}_\nu = \underline{R}_\nu \tag{4-16}$$

$$\underline{L}_{dq\nu} = \underline{\alpha}_{\nu}^{t} \, \underline{L}_{\nu} \, \underline{\alpha}_{\nu} =$$

$$= \begin{bmatrix} L_{ss} & 0 & L_{sr} & 0 \\ 0 & L_{ss} & 0 & L_{sr} \\ L_{rs} & 0 & L_{rr} & 0 \\ 0 & L_{rs} & 0 & L_{rr} \end{bmatrix}_{\nu} \qquad (4\text{-}17)$$

$$\underline{E}^{r}_{dq\nu} = \begin{bmatrix} 0 & 0 & 0 & 0 \\ 0 & 0 & 0 & 0 \\ 0 & \lambda L_{sr} & 0 & \lambda L_{rr} \\ -\lambda L_{sr} & 0 & -\lambda L_{rr} & 0 \end{bmatrix}_{\nu} \qquad (4\text{-}18)$$

Equation (4-15) now becomes

$$\begin{bmatrix} V_d^s \\ V_q^s \\ 0 \\ 0 \end{bmatrix} = \sum_{\nu=1}^{\infty} \left[\begin{array}{cc:cc} R_a^s + L_{ss}\,p & 0 & L_{sr}\,p & 0 \\ 0 & R_b^s + L_{ss}\,p & 0 & L_{sr}\,p \\ \hdashline L_{rs}\,p & \lambda L_{rs}\,\dot{x}^r & R_a^r + L_{ss}\,p & \lambda L_{rr}\,\dot{x}^r \\ -\lambda L_{rs}\,\dot{x}^r & L_{rs}\,p & -\lambda L_{rr}\,\dot{x}^r & R_b^r + L_{rr}\,p \end{array}\right]_{\nu} \begin{bmatrix} i_d^s \\ i_q^s \\ i_d^r \\ i_q^r \end{bmatrix}_{\nu} \qquad (4\text{-}19)$$

Equation (4-7) becomes

$$F^r_{e\nu} = \frac{1}{2} (\underline{\alpha}_\nu \underline{I}_{dq\nu})^t \underline{F}^r_{ab\nu} \underline{I}_{dq\nu} =$$

$$= \frac{1}{2} \underline{I}^t_{dq\nu} (\underline{\alpha}^t_\nu \underline{F}^r_{ab\nu} \underline{\alpha}_\nu) \underline{I}_{dq\nu} =$$

$$= \frac{1}{2} \underline{I}^t_{dq\nu} \underline{F}^r_{dq\nu} \underline{I}_{dq\nu}. \qquad (4\text{-}20)$$

or

$$F^r_{e\nu} = (i_q{}^s \; i_d{}^r - i_d{}^s \; i_q{}^r)_\nu \; \lambda_\nu \; L_{sr\nu} \qquad (4\text{-}21)$$

Equations (4-19) and (4-21) constitute the set of equations of motion of the machine.

4.3. Steady State Relationships

The fundamental slip is defined as

$$s_1 = \frac{v^s - v^r}{v^s} \qquad (4\text{-}22)$$

where

v^s - speed of the field

v^r - speed of the rotor

then

$$\lambda_\nu \dot{x}^r = \lambda_\nu v^r = \lambda_\nu v^s (1 - s_1) = \nu\omega^s (1 - s_1) =$$

$$= \omega^s [-(s_1\nu - \nu + 1 - 1)] = \omega^s (1 - s_\nu{}^r) \qquad (4\text{-}23)$$

For steady state

$$p = j\omega^s$$

and the v t-amp equations are

$$\begin{bmatrix} V_d^s \\ V_q^s \\ 0 \\ 0 \end{bmatrix}_\nu = \sum_{\nu=1}^{\infty} \left[\begin{array}{cc|cc} R_a^s + j\omega^s L_{ss} & 0 & j\omega^s L_{sr} & 0 \\ 0 & R_a^s + j\omega^s L_{ss} & 0 & j\omega^s L_{sr} \\ \hline j\omega^s L_{rs} & \omega^s(1-s_\nu^r)L_{sr} & R_a^r + j\omega^s L_{rr} & \omega^s(1-s_\nu^r)L_{rr} \\ -\omega^s(1-s_\nu^r)L_{sr} & j\omega^s L_{sr} & -\omega^s(1-s_\nu^r)L_{rr} & R_a^r + j\omega^s L_{rr} \end{array}\right]_\nu \begin{bmatrix} i_d^s \\ i_q^s \\ i_d^r \\ i_q^r \end{bmatrix}_\nu \tag{4-24}$$

Considering the steady state and balanced conditions, the stator currents $i_{a\nu}{}^s$ and $i_{b\nu}{}^s$ are in quadrature.

Let

$$v_a{}^s = v_d{}^s = V^s \cos \omega^s t$$

$$v_b{}^s = v_q{}^s = V^s \sin \omega^s t \tag{4-25}$$

In terms of complex exponentials, for sinusoidally varying voltages

$$\bar{V}^s = V^s e^{j0}$$

and

$$\bar{V}^s = \frac{1}{\sqrt{2}} (v_a{}^s + j\, v_b{}^s) \tag{4-26}$$

Similarly for the currents we have, dropping the subscripts,

$$\bar{I}^s = \frac{1}{\sqrt{2}} (i_a{}^s + j\, i_b{}^s) \tag{4-27}$$

$$\bar{I}^r = \frac{1}{\sqrt{2}} (i_d{}^r + j\, i_q{}^r) \tag{4-28}$$

The force equations become

$$F_{e\nu}{}^r = 2\, \lambda_\nu\, L_{sr\nu}\ \ \mathrm{Im}[\bar{I}^r\, \bar{I}^{s*}] \tag{4-29}$$

The volt-amp equations are

$$\begin{bmatrix} \bar{V}^s \\ 0 \end{bmatrix} = \sum_{\nu=1}^{\infty} \begin{bmatrix} R_a^s + j\omega^s L_{ss} & j\omega^s L_{sr} \\ j\omega^s L_{rs} s^r & R_a^r + j\omega^s L_{rr} s^r \end{bmatrix}_\nu \begin{bmatrix} \bar{I}^s \\ \bar{I}^r \end{bmatrix}_\nu \tag{4-30}$$

or, replacing $j\omega^s L_{ss}$ by $j X_{ss}$, $j\omega^s L_{sr}$ by $j X_{ss}$, $j\omega^s L_{rs}$ by $j X_{rs}$ and $j\omega^s L_{rr}$ by $j X_{rr}$, we have

$$\begin{bmatrix} \bar{V}^s \\ 0 \end{bmatrix} = \sum_{\nu=1}^{\infty} \begin{bmatrix} R_a^s + j X_{ss} & j X_{sr} \\ j X_{rs} & \frac{R_a^r}{s} + j X_{rr} \end{bmatrix}_\nu \begin{bmatrix} \bar{I}^s \\ \bar{I}^r \end{bmatrix}_\nu \tag{4-31}$$

where

$$s_\nu = 1 - \nu + \nu s_1 \qquad \text{forward harmonic slip}$$

$$s_{\nu'} = 1 + \nu - \nu s_1 \qquad \text{backward harmonic slip} \qquad (4\text{-}32)$$

4.4. Equivalent Circuit

Equations (4-31) can be represented by the equivalent circuit shown in Fig. 4-1.

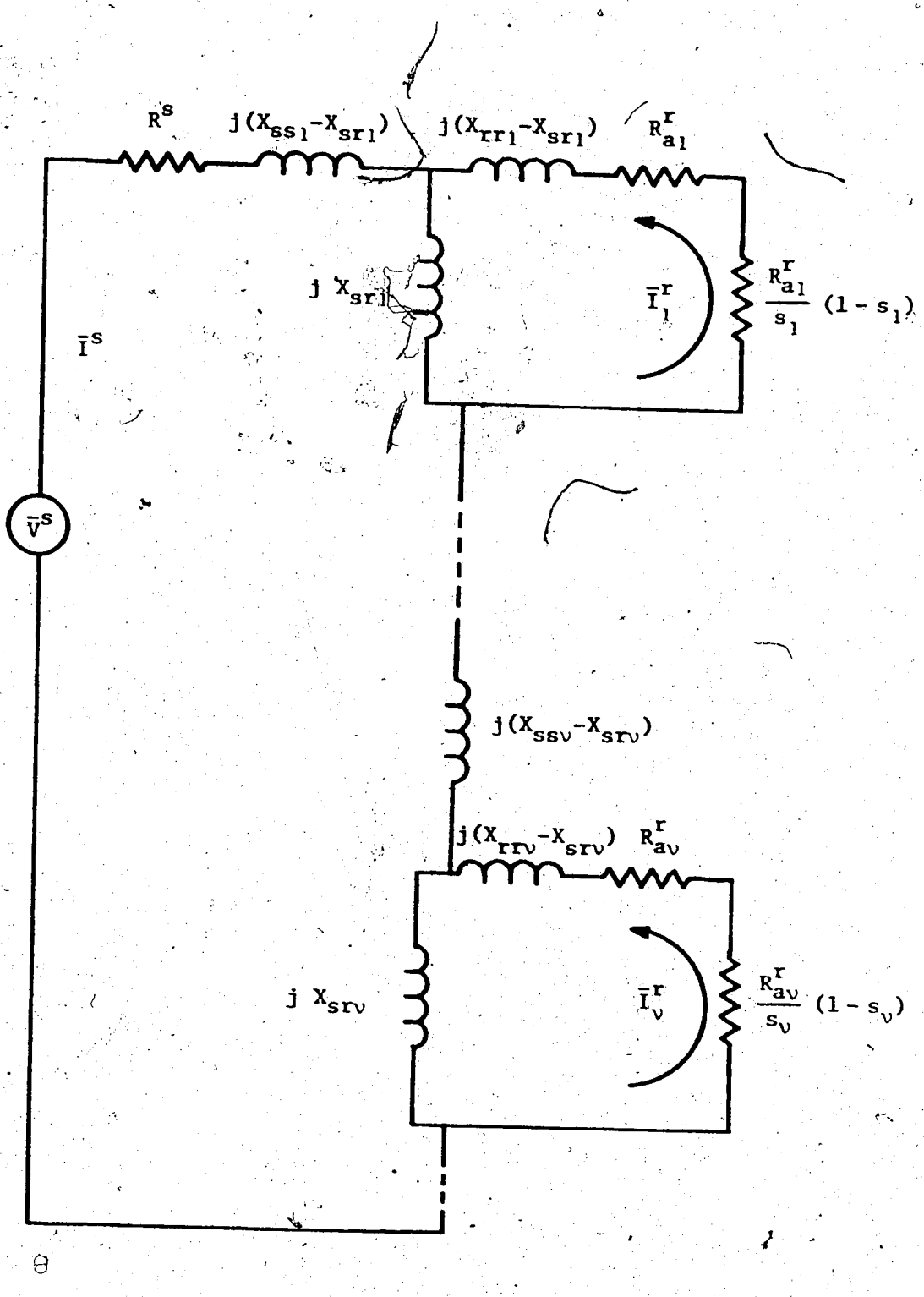

FIG. 4-1 EQUIVALENT CIRCUIT - STEADY STATE

CHAPTER V

DIGITAL STUDIES OF THE MOTOR

The entry and exit edge effect of the machine are neglected, therefore calculations of the machine performance are based on the straightforward use of equations (3-9), (3-11), (3-14), (4-29) and (4-31).

5.1. Force Equations

Harmonic forces can be derived with the help of the equivalent circuit or directly from equations (4-31) and (4-29), giving the same result.

The total impedance of the equivalent circuit is

$$z = \text{Real} + j\ \text{Imag} \tag{5-1}$$

where

$$\text{Real} = R^s + \frac{\frac{R^r_{al}}{s_1} X^2_{sr1}}{\left(\frac{R^r_{al}}{s_1}\right)^2 + X^2_{rr1}} + \cdots + \frac{\frac{R^r_{a\nu}}{s_\nu} X^2_{sr\nu}}{\left(\frac{R^r_{a\nu}}{s_\nu}\right)^2 + X^2_{rr\nu}} + \cdots \tag{5-2}$$

and

$$\text{Imag} = X_{ss1} + \cdots + X_{ss\nu} + \cdots - \frac{X^2_{sr1} X_{rr1}}{\left(\frac{R^r_{al}}{s_1}\right)^2 + X^2_{rr1}} - \cdots - \frac{X^2_{sr\nu} X_{rr\nu}}{\left(\frac{R^r_{a\nu}}{s_\nu}\right)^2 + X^2_{rr\nu}} - \cdots \tag{5-3}$$

The k^{th} harmonic rotor current is given by

$$\bar{I}^r_k = \frac{-\,j\,X_{srk}\left(\frac{R^r_{ak}}{s_k} - j\,X_{rrk}\right)\bar{V}^s}{\left[\left(\frac{R^r_{ak}}{s_k}\right)^2 + X^2_{rrk}\right]\left[\text{Real} + j\,\text{Imag}\right]} \qquad (5\text{-}4)$$

and the k^{th} harmonic force by

$$F^r_{ek} = \frac{2\,\lambda_k\,L_{srk}\,X_{srk}\,\frac{R^r_{ak}}{s_k}\,|\bar{V}^s|^2}{\left[\left(\frac{R^r_{ak}}{s_k}\right)^2 + X^2_{rrk}\right]\left[\text{Real}^2 + \text{Imag}^2\right]} \qquad (5\text{-}5)$$

The total force on the rotor is obtained by summing the harmonic forces (5-5)

$$F^r_e = \sum_{k=1}^{\infty} F^r_{ek} \qquad (5\text{-}6)$$

In general, some of the spatial harmonics of the current densities are negative, creating backward travelling magnetic fields, therefore the corresponding harmonic forces in (5-6) are reversed.

5.2. Efficiency

The performance of the machine was computed on a digital computer, using the APL program language. The machine data are listed in Appendix C-1.

Efficiencies are calculated, using the following equations:

$$\text{Stator copper loss} = R_a^s (I^s)^2$$

$$\text{Rotor Cu (Al) loss} = \sum_{\nu=1}^{n} R_{a\nu}^r (I_\nu^r)^2$$

$$\text{Developed power} = \sum_{\nu=1}^{n} \frac{R_{a\nu}^r}{s_\nu} (1 - s_\nu)$$

$$\text{Efficiency} = \frac{\text{power output}}{\text{power output + losses}} \qquad (5\text{-}7)$$

Hysteresis and iron losses as well as mechanical losses of the motor are not included.

Winding distribution factors for different types of stator windings, digital programs and inductances are listed in Appencix C.

CHAPTER VI

RESULTS AND DISCUSSIONS

6.1. Outline

The steady state output characteristics of a tubular motor were computed, using the program in Table 2, Appendix C. The program holds for an infinitely long machine. As a tubular motor would operate at higher slips, the entry and exit effects are negligible (20) as both the forward and backward travelling waves caused by the reflection at the edges decay rapidly.

The effect of different winding distribution factors, air gap thickness and rotor sleeve thickness on machine characteristics is studied in this chapter.

The calculations are done for three stators, each having different winding distribution. They are type I, type II and type III stator windings, as described in Appendix C-2. Thickness of the winding is given by the value of $|y_3 - y_2|$ in centimetres. A set of different rotors is considered, each having different thickness of the copper rotor sleeve. Another similar set of rotors has aluminum sleeves. The thickness of the rotor sleeve is described by the value of y_1 in centimetres. The clearance, i.e. the air gap between the rotor sleeve and the stator winding is $|y_2 - y_1|$ and is also in centimetres.

The machine data are listed in Appendix C. The temperature of both the stator and rotor conductors is assumed to be 75°C.

6.2. Effect of Winding Distribution Factors

In Figs. 6-1, 6-2 and 6-3 steady state output forces, efficiencies and stator currents are plotted.

Fig. 6-1 compares output forces for three different stators and the rotor with the sleeve 0.2 cm thick. The characteristics for the copper rotor sleeve show an increase in output forces as the stator windings type II and type III are considered. The type III curve reaches a maximum for slip $s > 1$. The aluminum rotor sleeve has higher rotor resistances, therefore the force maxima occur at slips $s > 1$.

Fig. 6-2 shows the effect of stator distribution factors on efficiencies. For the same type of stator winding, the efficiency is higher for the machine with the copper rotor sleeve over one with the aluminum sleeve as the rotor losses are smaller for the copper sleeve. The efficiency of the type III machine is higher than the efficiency of the type II machine, which is higher than the type I machine efficiency, as the distribution of magnetic fields in the air gap is improved.

Fig. 6-3 shows the stator currents of the machine. The highest currents are for the type I machine, the lowest for the type III machine.

The performance of the machine was considerably improved by the type II stator winding and was the best for the type III stator winding, as the direct result of the improved distribution of the magnetic fields within the air gap, the distribution being more sinusoidal.

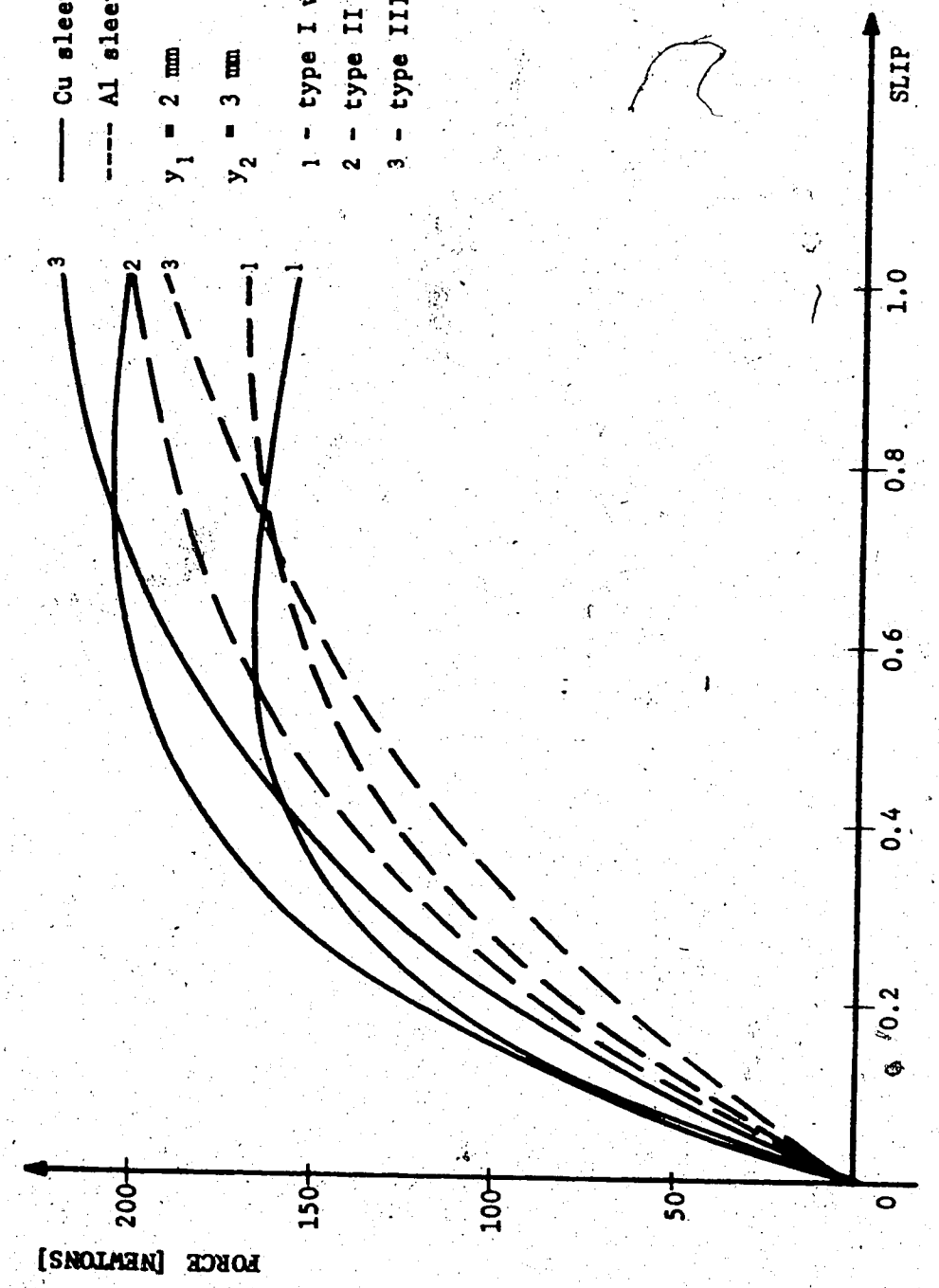

FIG. 6-1 OUTPUT FORCES - WINDING DISTRIBUTION EFFECT

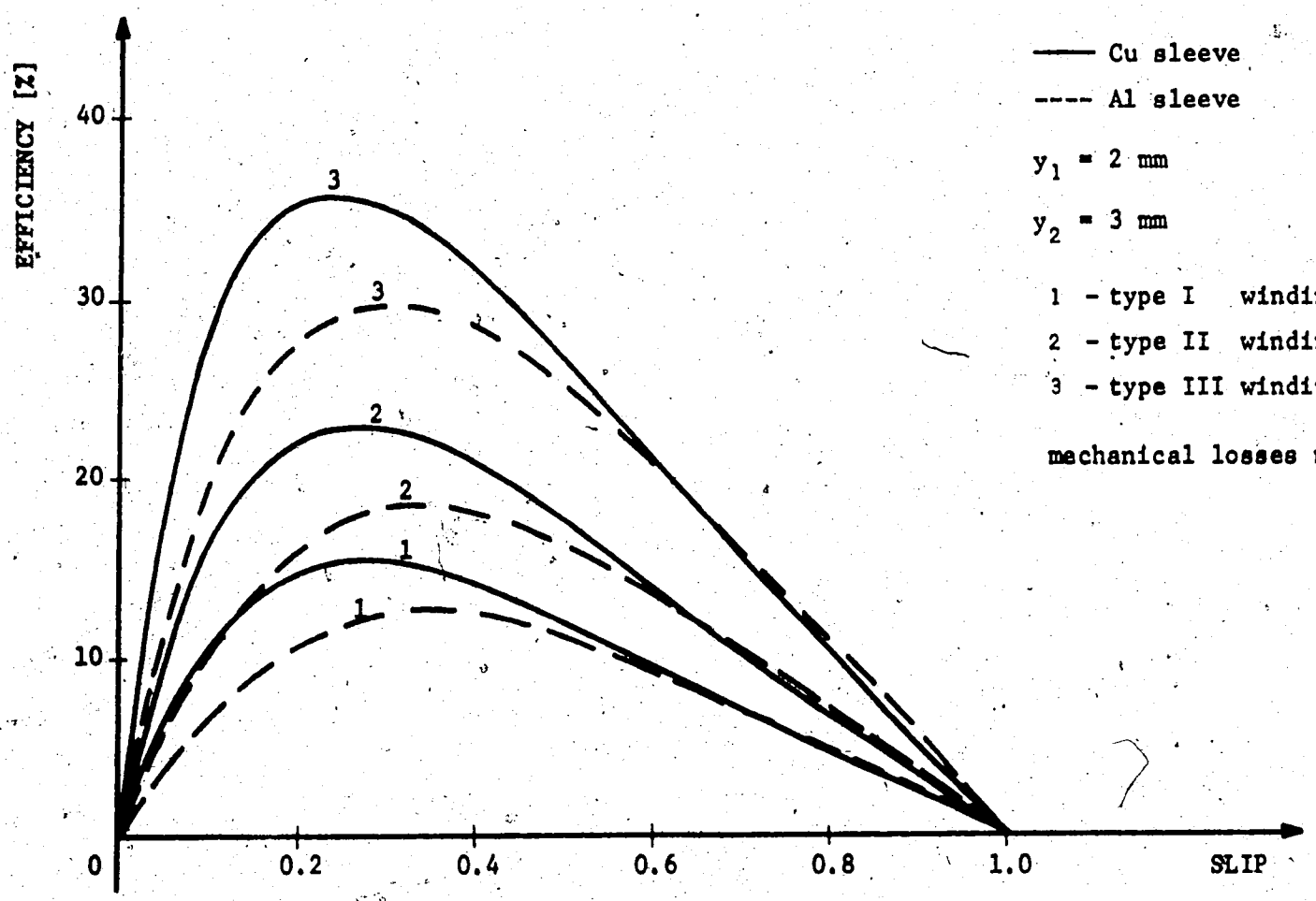

FIG. 6-2 EFFICIENCIES

FIG. 6-3 STATOR CURRENTS

The following data were used:

$$y_1 = 0.2 \text{ cm}, \quad y_2 = 0.3 \text{ cm}$$

Figs. 6-4, 6-5 and 6-6 are similar to those considered in the above example. The thickness of the rotor sleeve was increased, thus the air gap y_3 was also increased. The rotor resistances decreased, therefore the force maxima occur at lower slip. The machine performance is as described above. The data used are

$$y_1 = 0.3 \text{ cm}, \quad y_2 = 0.4 \text{ cm}$$

Fig. 6-7 compares the first harmonic force with the total force, the difference is less than 3% for slips higher than 0.2. This is for the machine with the type I stator winding distribution. The overall effect of the higher harmonics is small and the total force is smaller than the first harmonic force. The effect of higher harmonic forces for the type II and type III windings was much smaller than for the type I winding.

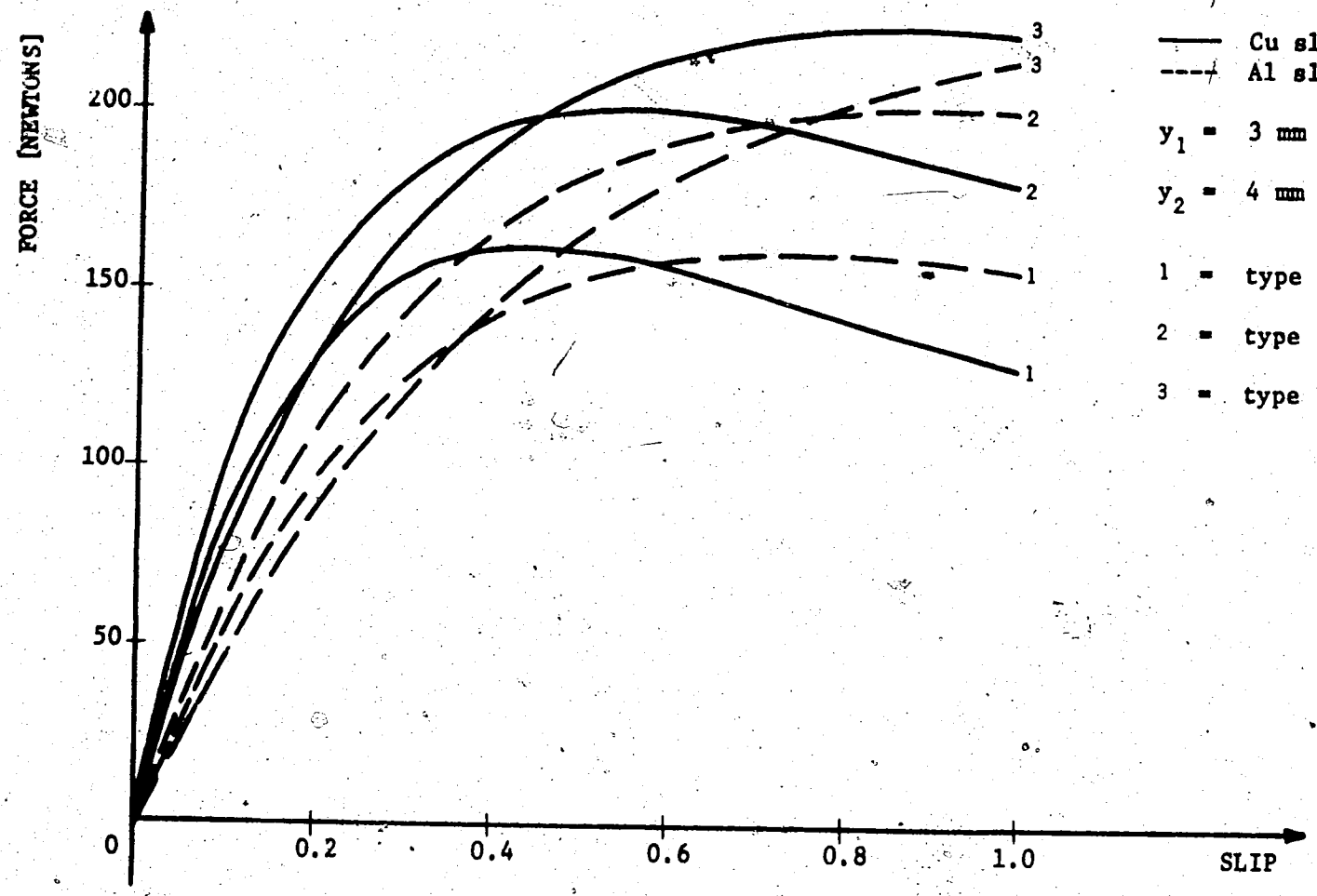

FIG. 6-4 OUTPUT FORCES - WINDING DISTRIBUTION EFFECT

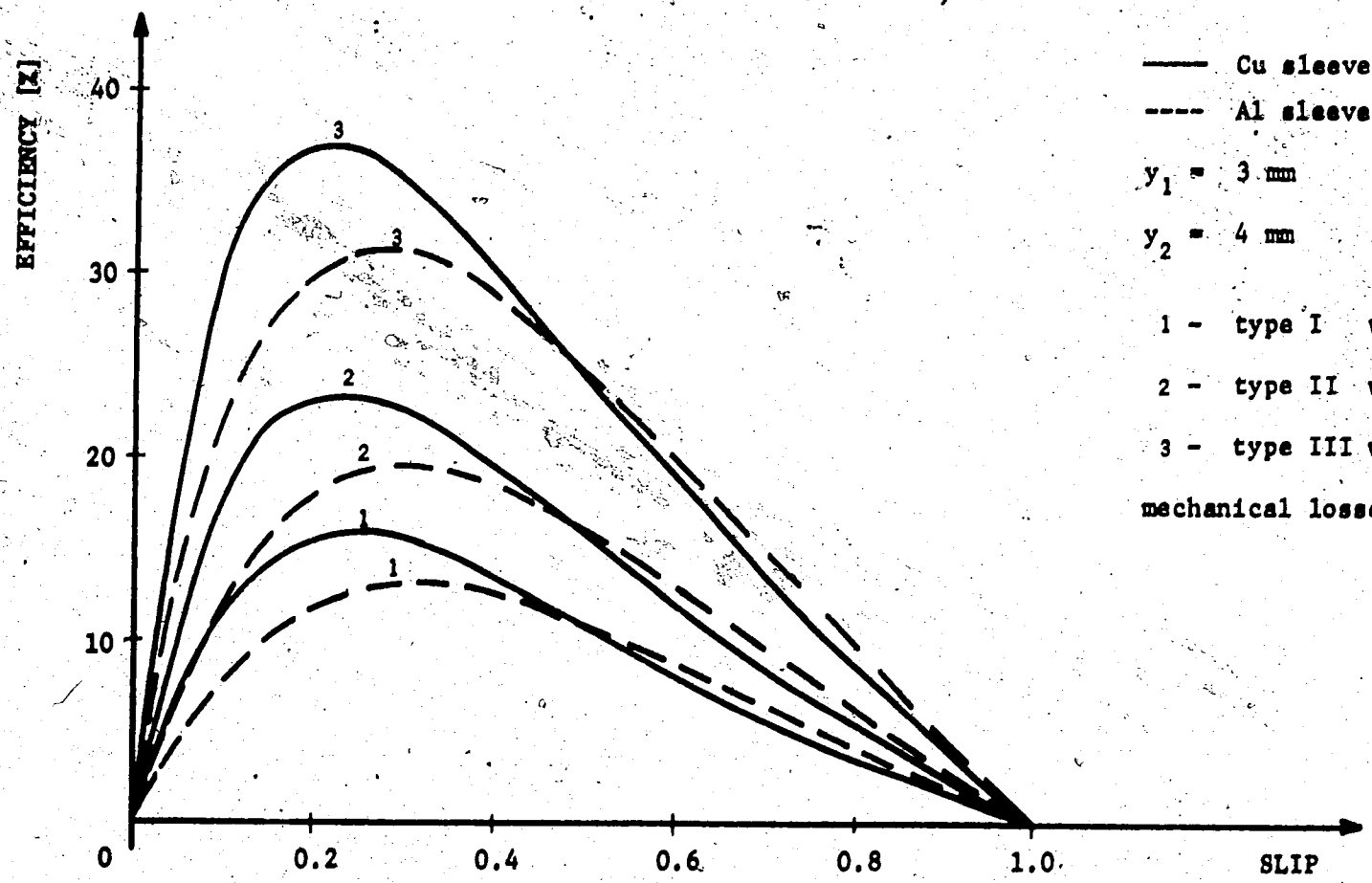

FIG. 6-5 EFFICIENCIES

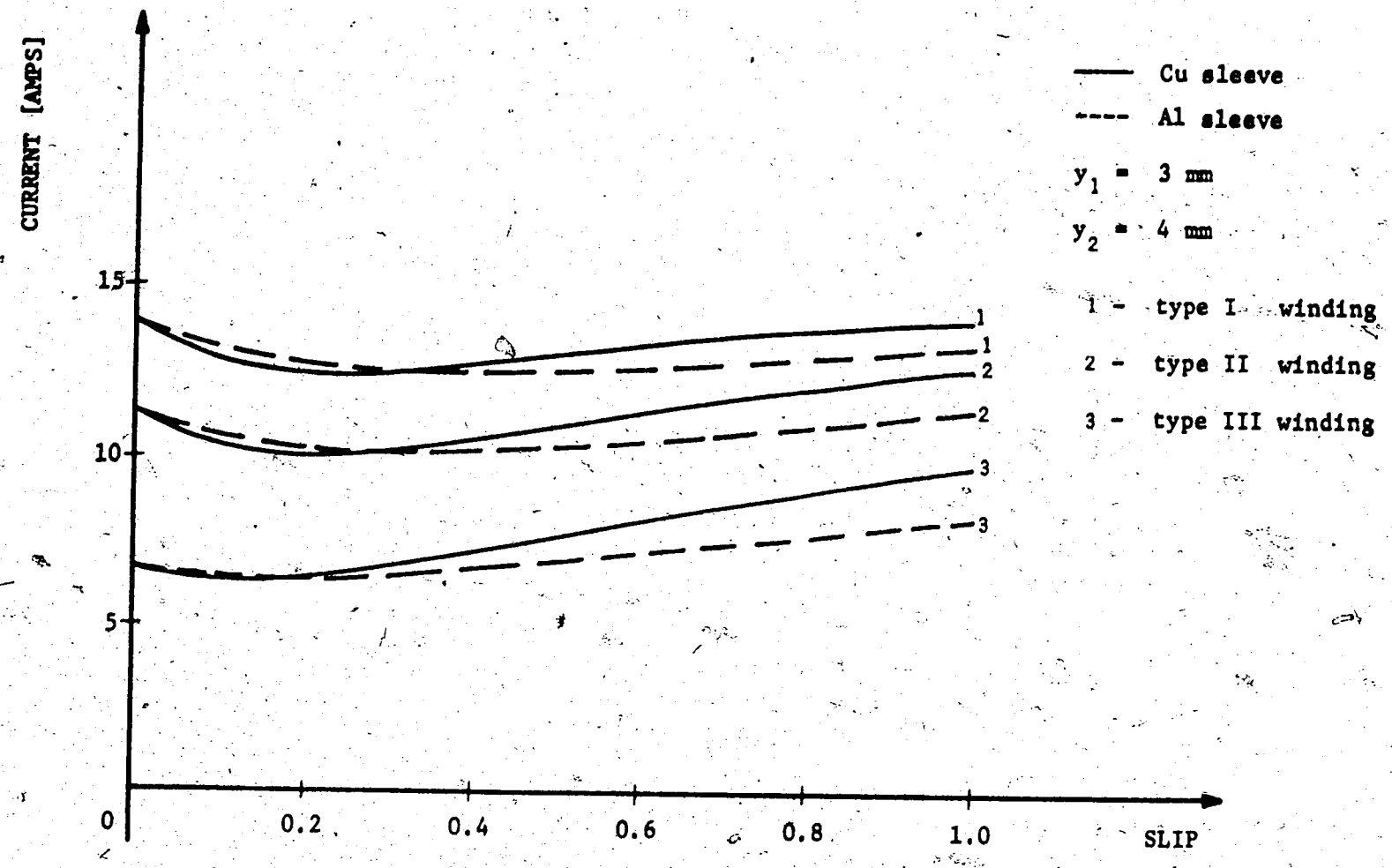

FIG. 6-6 STATOR CURRENTS

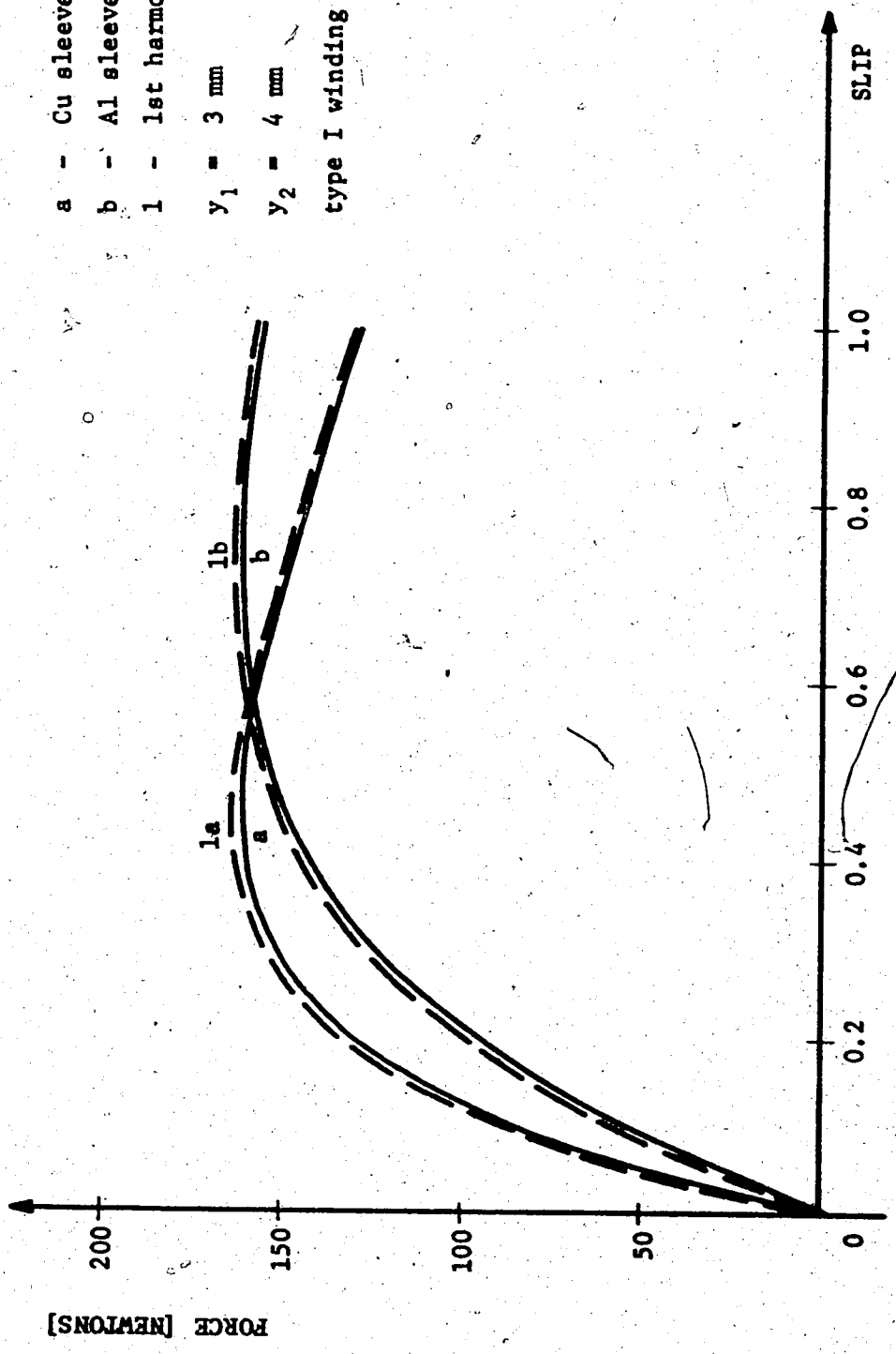

FIG. 6-7 FIRST HARMONIC FORCES

6.3. Effect of Air Gap Thickness

In the next example only the winding type I is taken into consideration, as it is the simplest to make. The air gap thickness $|y_2 - y_1|$, which is actually the clearance between the stator and rotor conductors, was assigned different values and the program in Table 2, Appendix C, was used for computations.

Fig. 6-8 shows the effect of variations of the air gap on the output forces both for copper and aluminum rotor sleeves. An increase of the air gap width causes a decrease of the output forces. This is due to the increase of the leakage of the magnetic fields within the air gap. The curves corresponding to the aluminum rotor sleeve have the peak forces near standstill due to higher resistances.

The efficiency characteristics for the tubular motor with the copper rotor sleeve are shown in Fig. 6-9 and with the aluminum sleeve in Fig. 6-10. The decrease of the efficiency is considerable except for speeds close to standstill.

The stator currents are plotted in Figs. 6-11 and 6-12. The increase in the air gap width decreases the inductances as can be seen from equations (3-13). This means that the total impedance of the machine is smaller, therefore the stator currents are larger as the terminal voltage is constant. Furthermore, the leakage inductances are increased as the air gap width is increased. The magnetizing inductances are decreased, therefore requiring higher magnetizing currents.

The machine performance is considerably affected by the increase of the air gap, as both the output forces and efficiencies are decreased and the stator currents are increased.

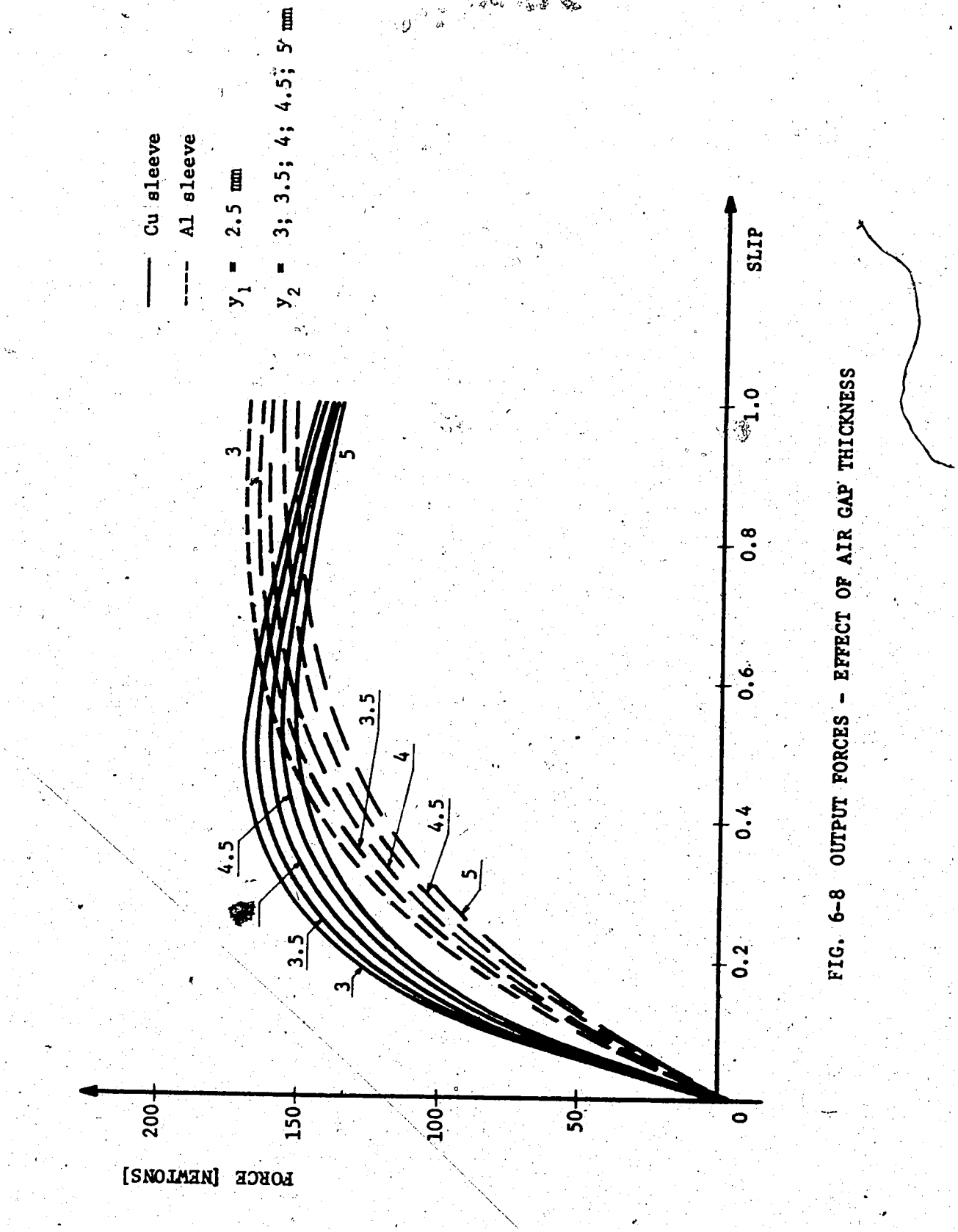

FIG. 6-8 OUTPUT FORCES - EFFECT OF AIR GAP THICKNESS

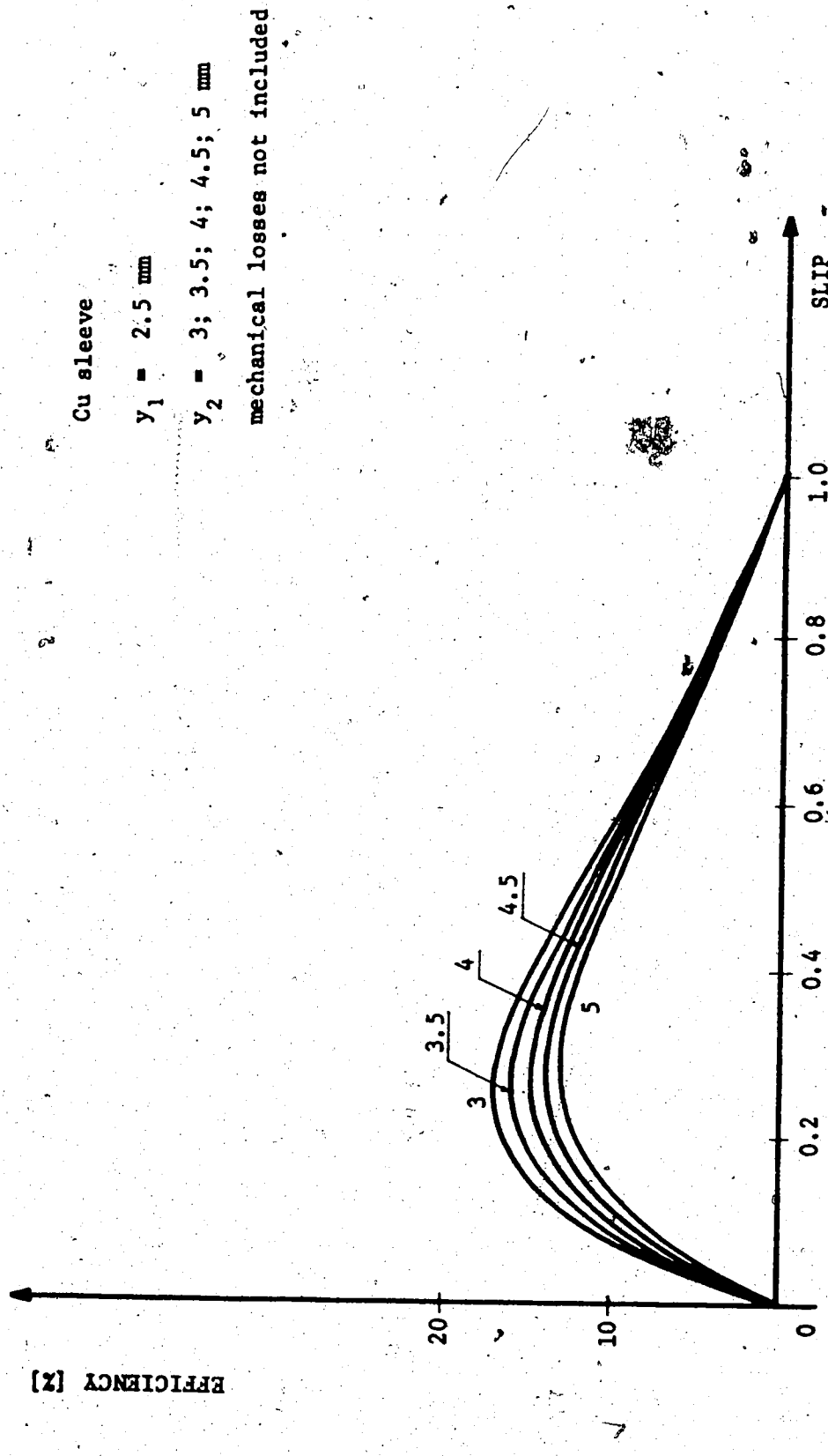

FIG. 6-9 EFFICIENCIES (copper rotor sleeve)

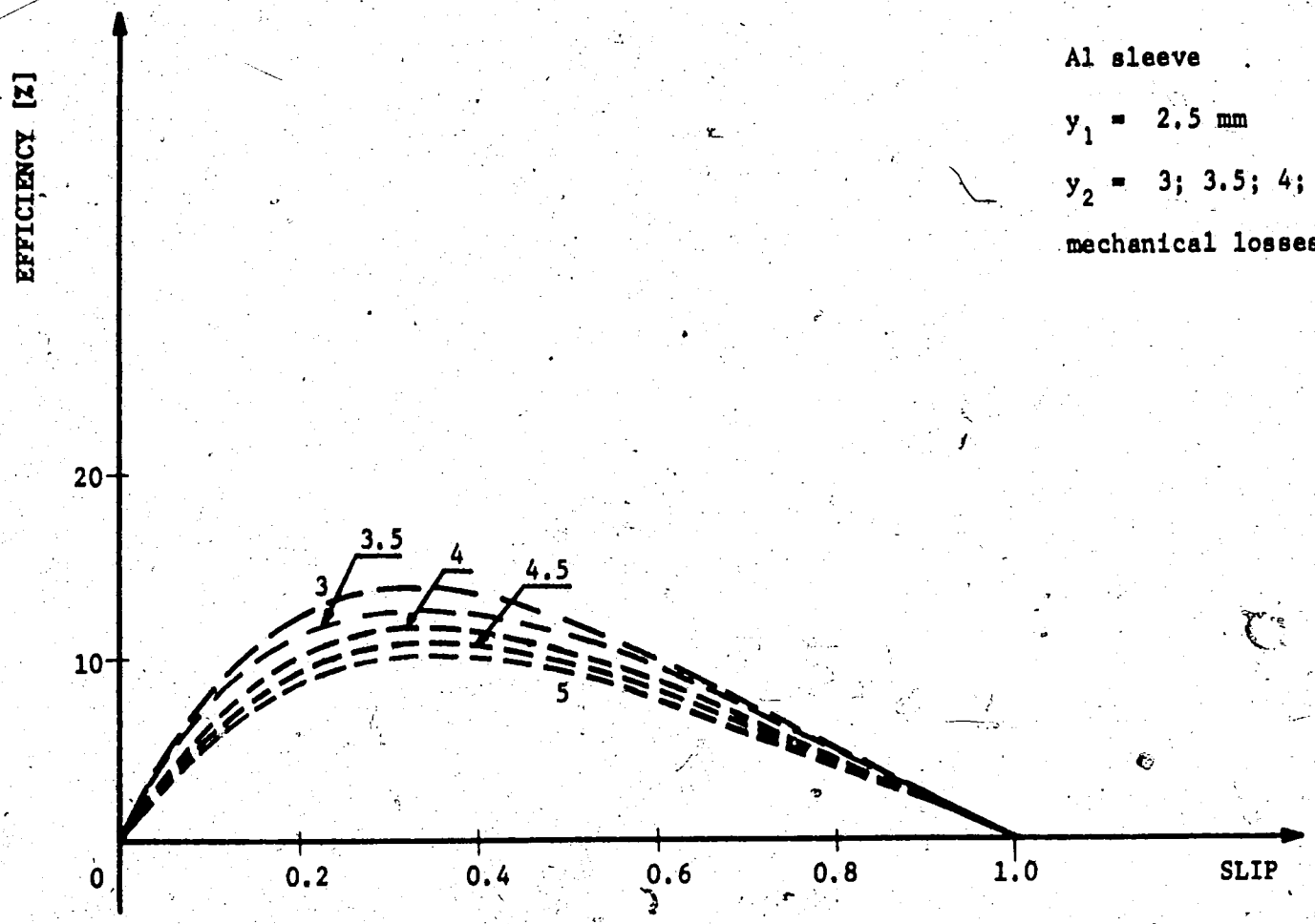

FIG. 6-10 EFFICIENCIES (aluminum rotor sleeve)

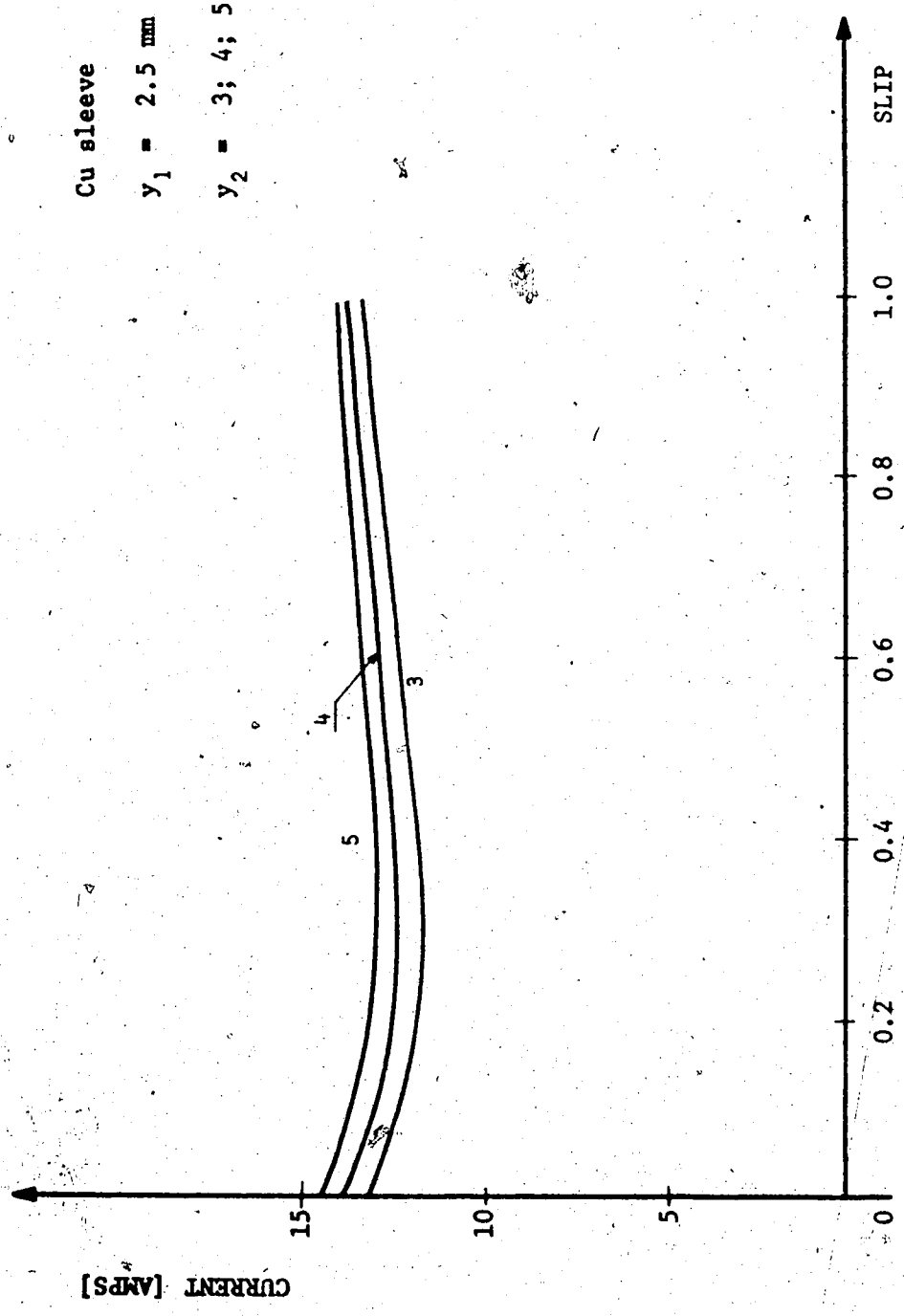

FIG. 6-11 STATOR CURRENTS (copper rotor sleeve)

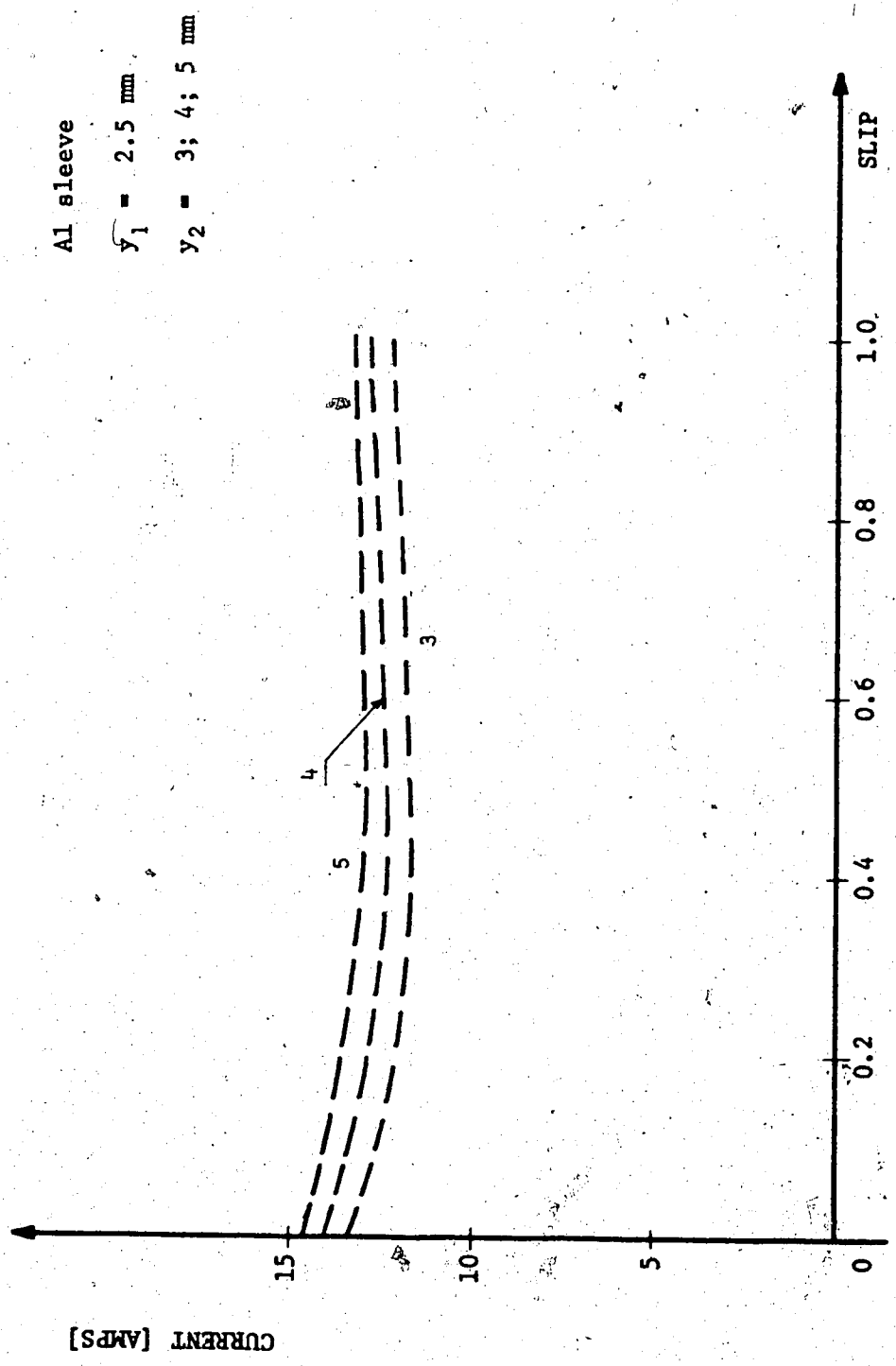

FIG. 6-12 STATOR CURRENTS (aluminum rotor sleeve)

6.4. Effect of Rotor Thickness

Next the set of tubular motors, having the constant air gap y_3 and variable rotor thickness y_1, is considered. Fig. 6-13 and Fig. 6-14 show the output forces for copper and aluminum sleeves respectively. For small slips the forces are increased, for higher slips they are smaller. The efficiency characteristics (Fig. 6-15 and Fig. 6-16) and stator currents (Fig. 6-17 and Fig. 6-18) are affected in a similar way as the forces.

The increase of forces and efficiencies is the result of increased rotor conductivity. As the slip increases, the effect of increased leakage inductances is larger and the forces and efficiencies decrease. This is more apparent with the copper rotor sleeve than with the aluminum rotor sleeve with higher resistivity.

The tubular motor employing rotors with different thickness of the sleeves, has better force and efficiency characteristics at higher speeds of the rotor. As the direct result of increased rotor leakage inductances for small slips, the increase of the rotor sleeve thickness causes the decrease of the output forces and efficiencies. For small slips the machine performs better, as the effect of higher conductivities is bigger than the effect of increased rotor leakage inductances.

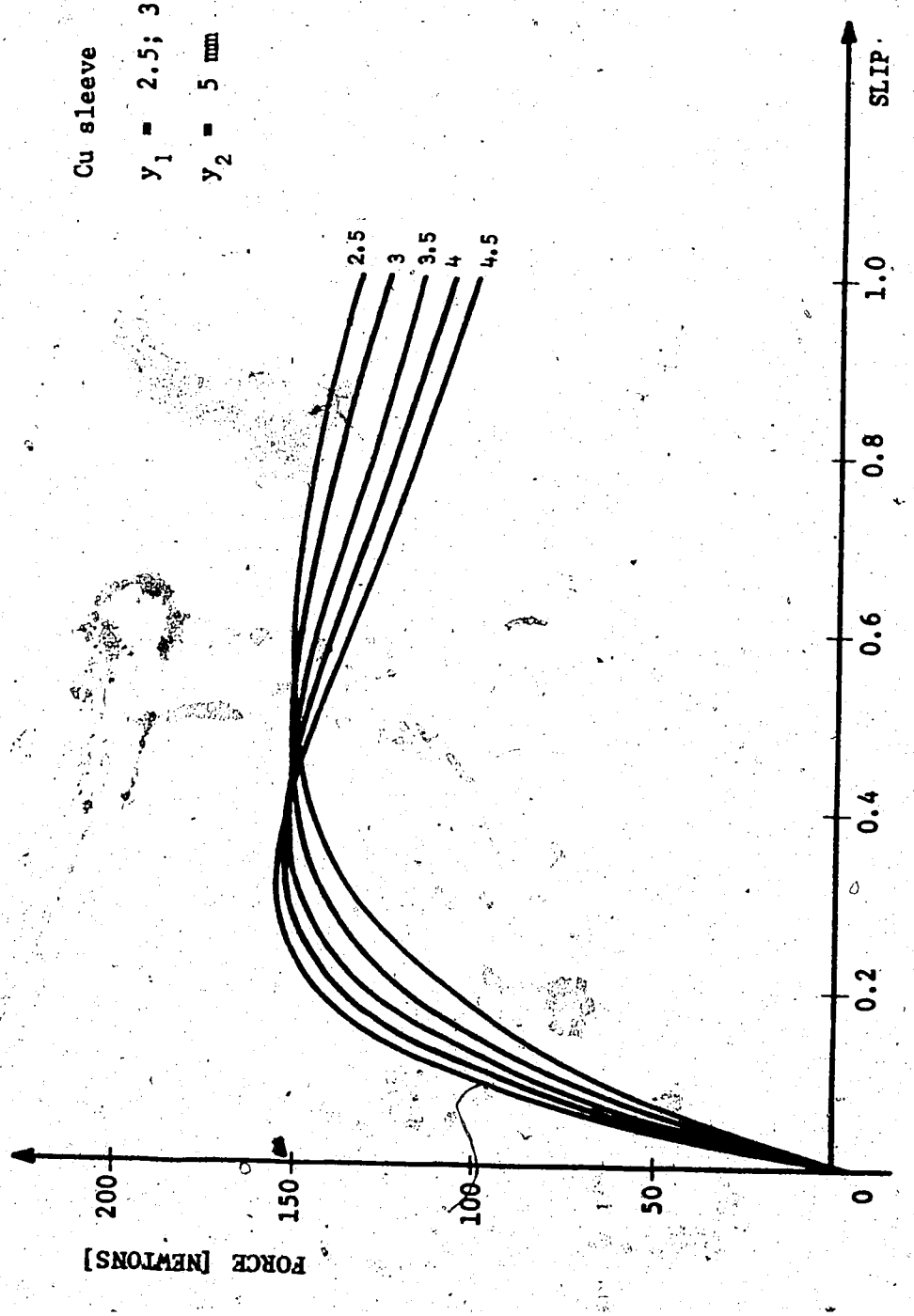

FIG. 6-13 OUTPUT FORCES - EFFECT OF ROTOR THICKNESS

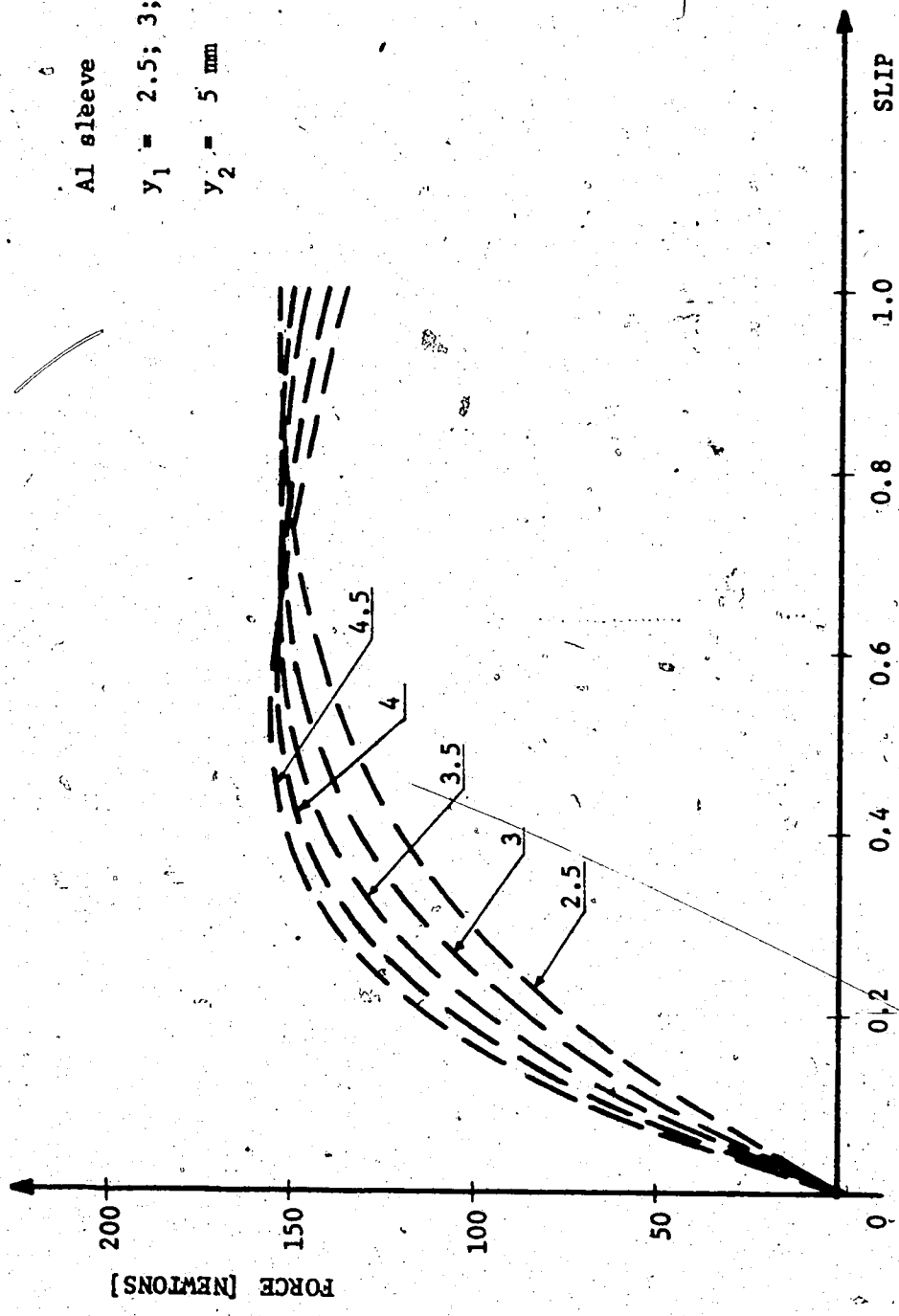

FIG. 6-14 OUTPUT FORCES

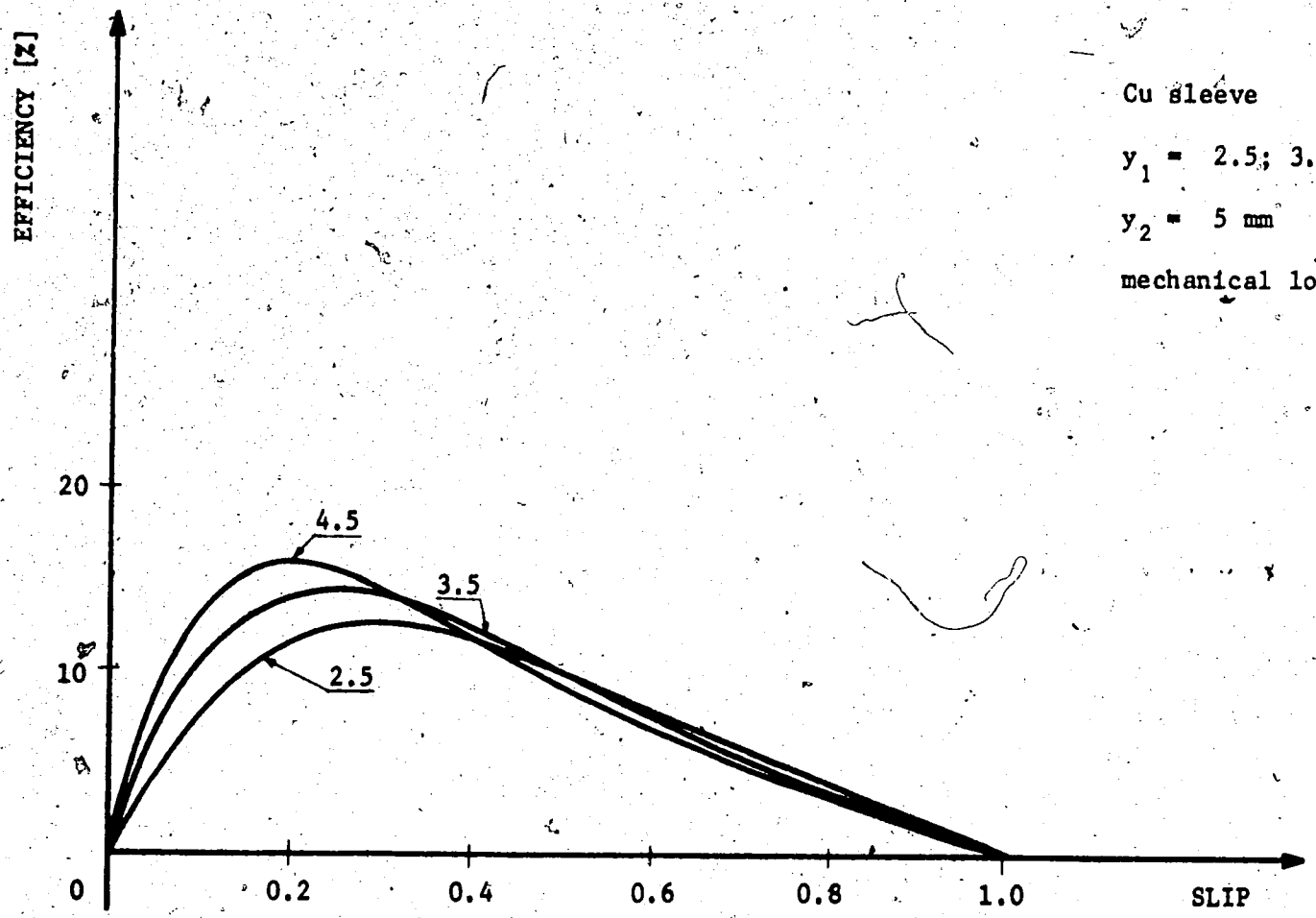

Cu sleeve

y_1 = 2.5; 3.5; 4.5 mm

y_2 = 5 mm

mechanical losses not included

FIG. 6-15 EFFICIENCY

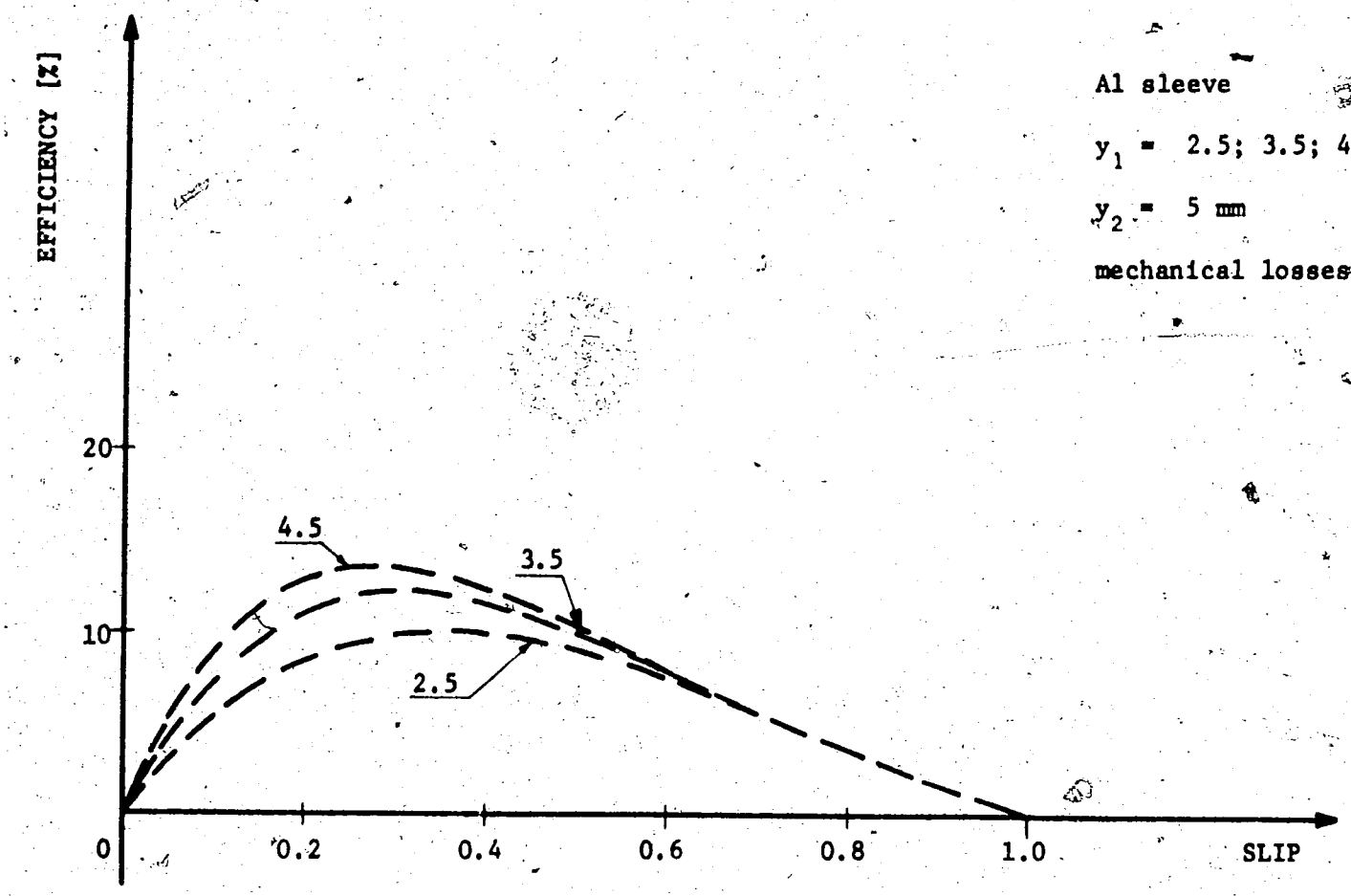

FIG. 6-16 EFFICIENCY

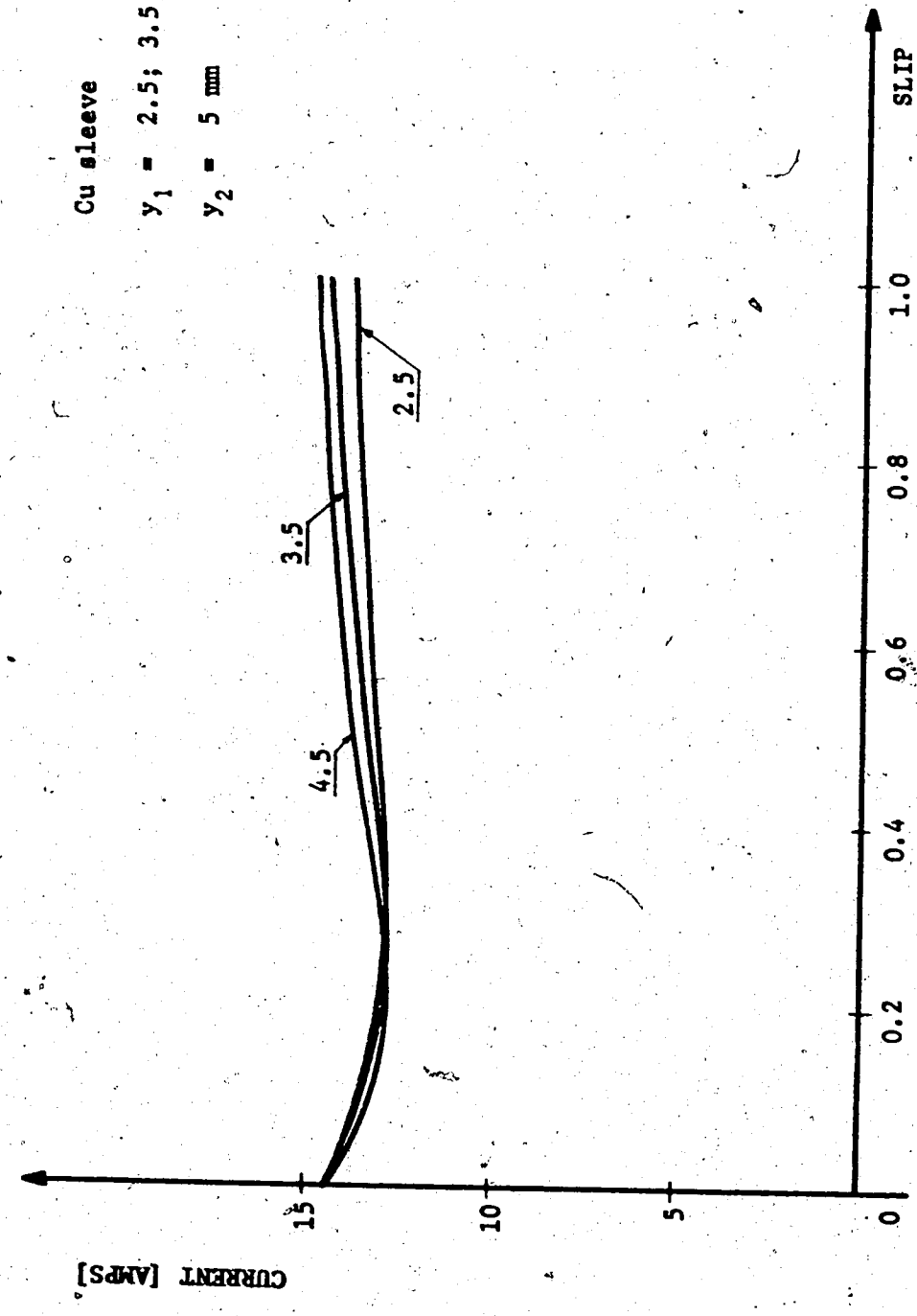

FIG. 6-17 STATOR CURRENTS

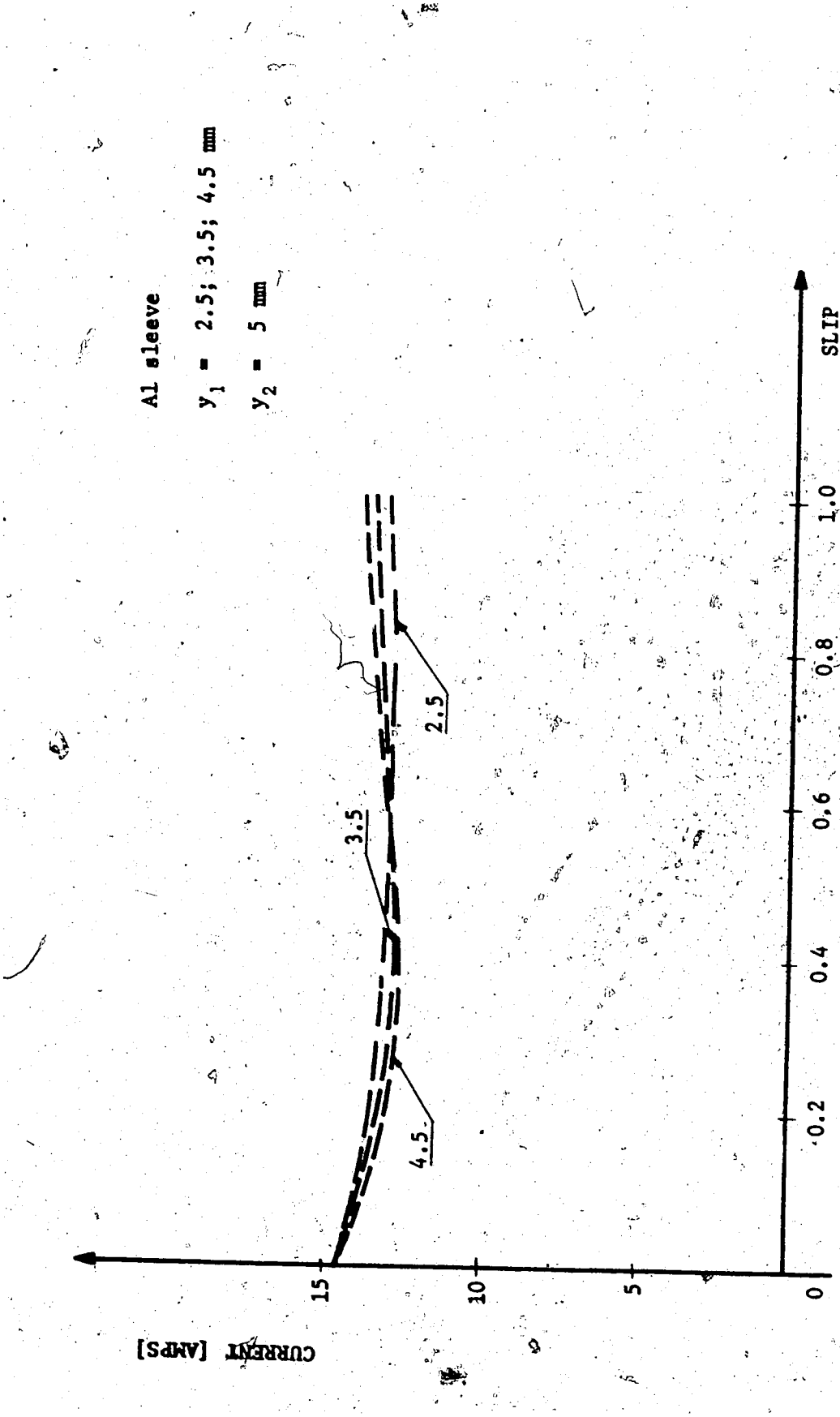

FIG. 6-18 STATOR CURRENTS

6.5. Constant Clearance

Next, for practical purposes, the air gap clearance $|y_2 - y_1|$ between the windings is kept constant. The effect of the rotor conductor thickness is considered for the type I stator windings. This means that an increase of the sleeve thickness causes a corresponding increase of the total air gap thickness, thus the effect of both on the machine performance is combined. The air gap clearance is 0.1 cm.

The output forces are plotted in Fig. 6-19 for copper sleeves and in Fig. 6-20 for aluminum sleeves. An increase of the sleeve thickness causes an increase of output forces for small slips and a decrease of the forces for higher slips. The decrease is caused by the increase of the leakage inductances.

The efficiency curves in Fig. 6-21 and Fig. 6-22 show some increase in efficiency for small slips and decrease for higher slips, being the result of a combination of rotor sleeve resistances and leakage inductance. Fig. 6-23 and Fig. 6-24 show an increase of stator currents as the sleeve thickness is increased and consequently the total impedance of the machine is decreased, as the increase of leakage inductances has a smaller effect than the increase of the conductivity.

The machine performance is affected for the higher slips, being decreased especially for the machine with the copper rotor sleeve. Therefore, an increase of the sleeve thickness, while the clearance is kept constant, results in a machine with inferior output characteristics.

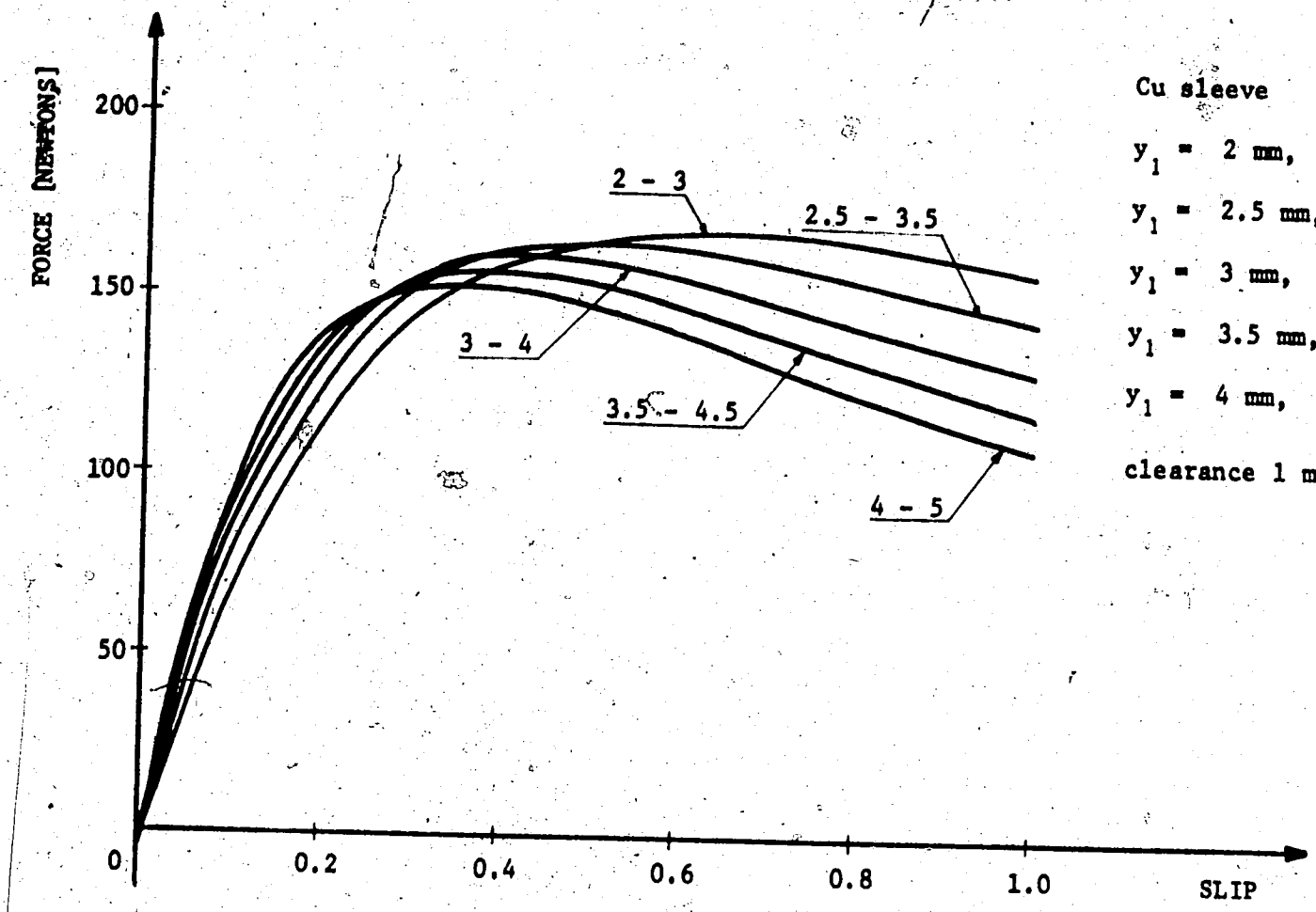

FIG. 6-19 OUTPUT FORCES - CONSTANT CLEARANCE

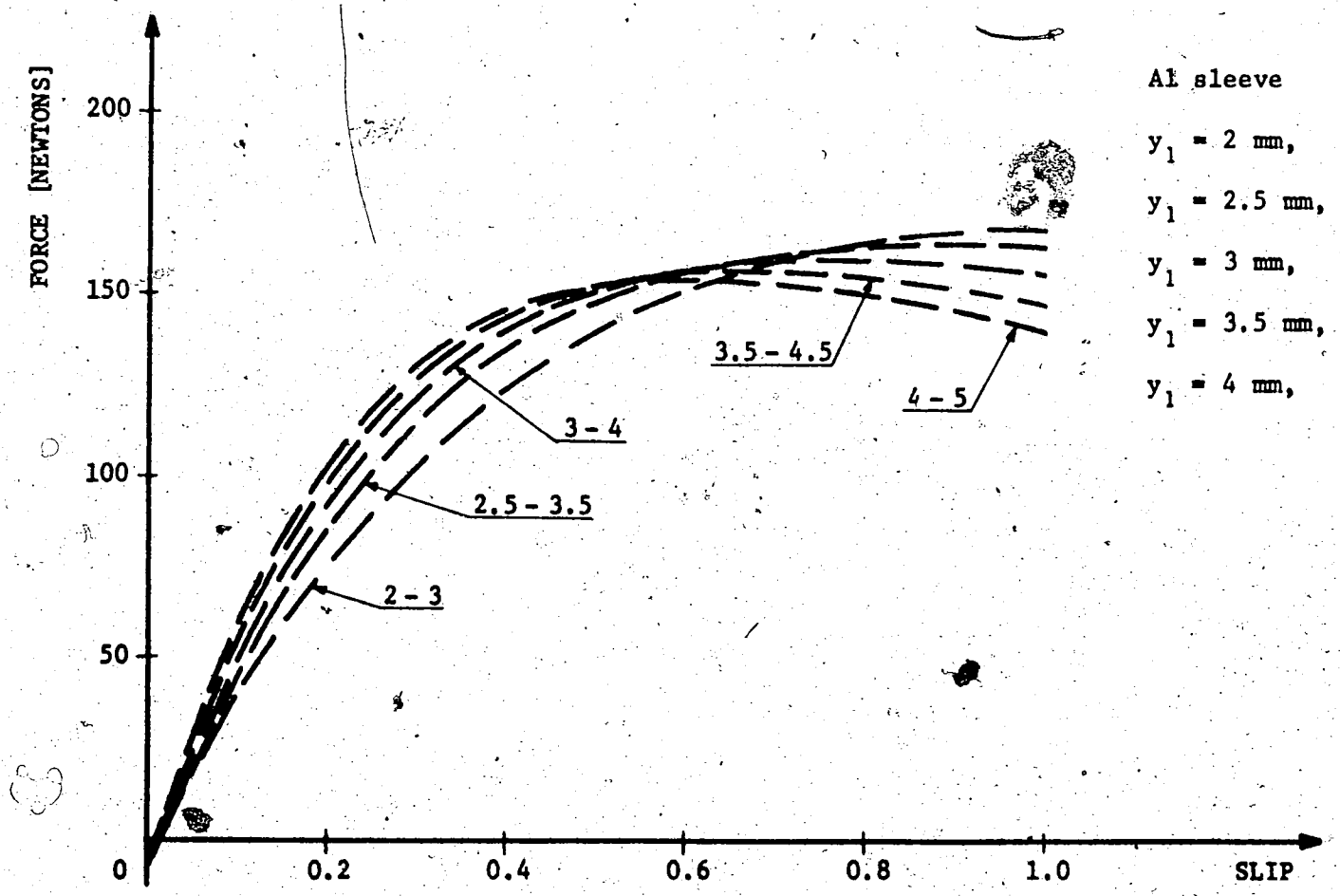

FIG. 6-20 OUTPUT FORCES

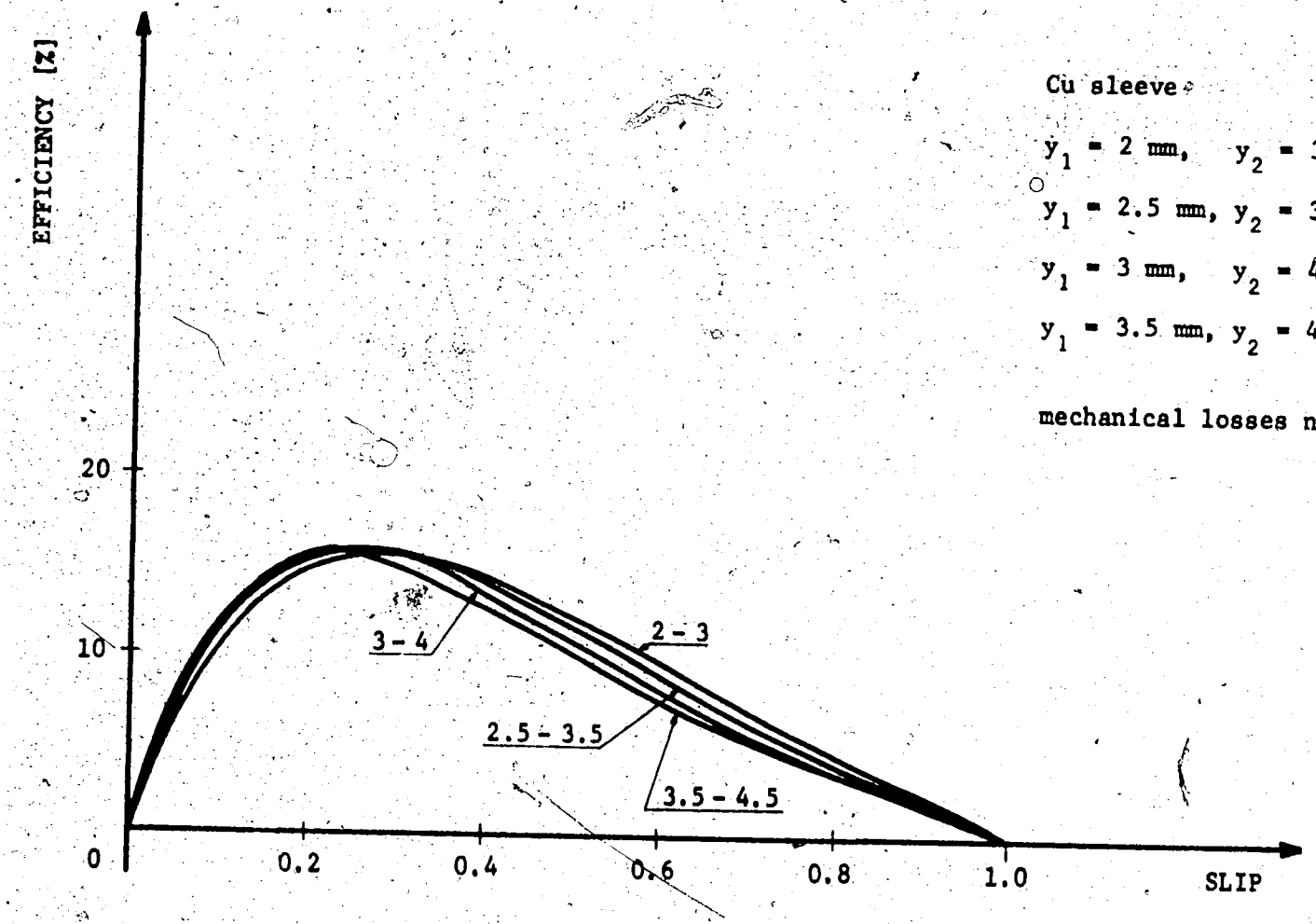

FIG. 6-21 EFFICIENCIES

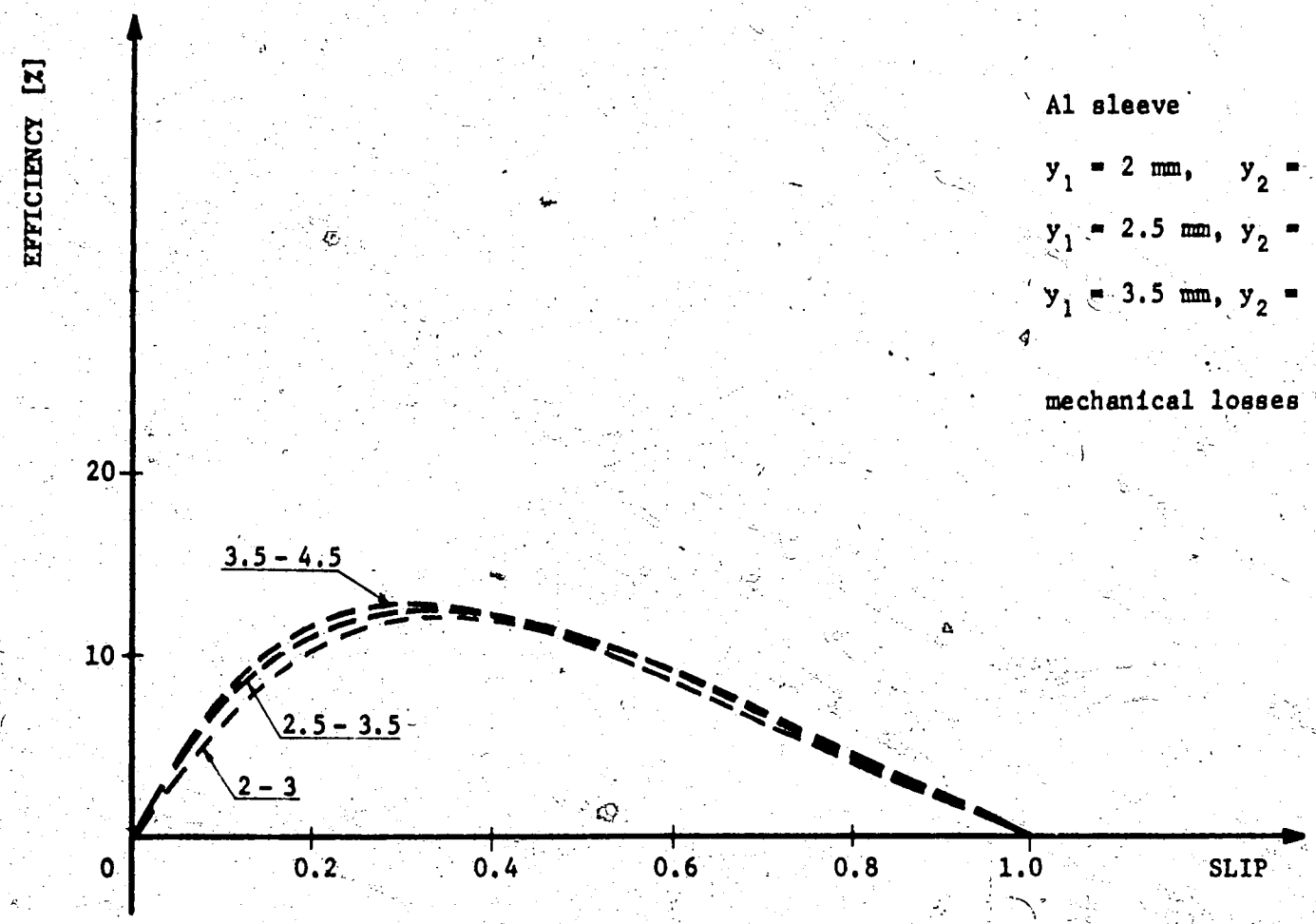

FIG. 6-22 EFFICIENCIES

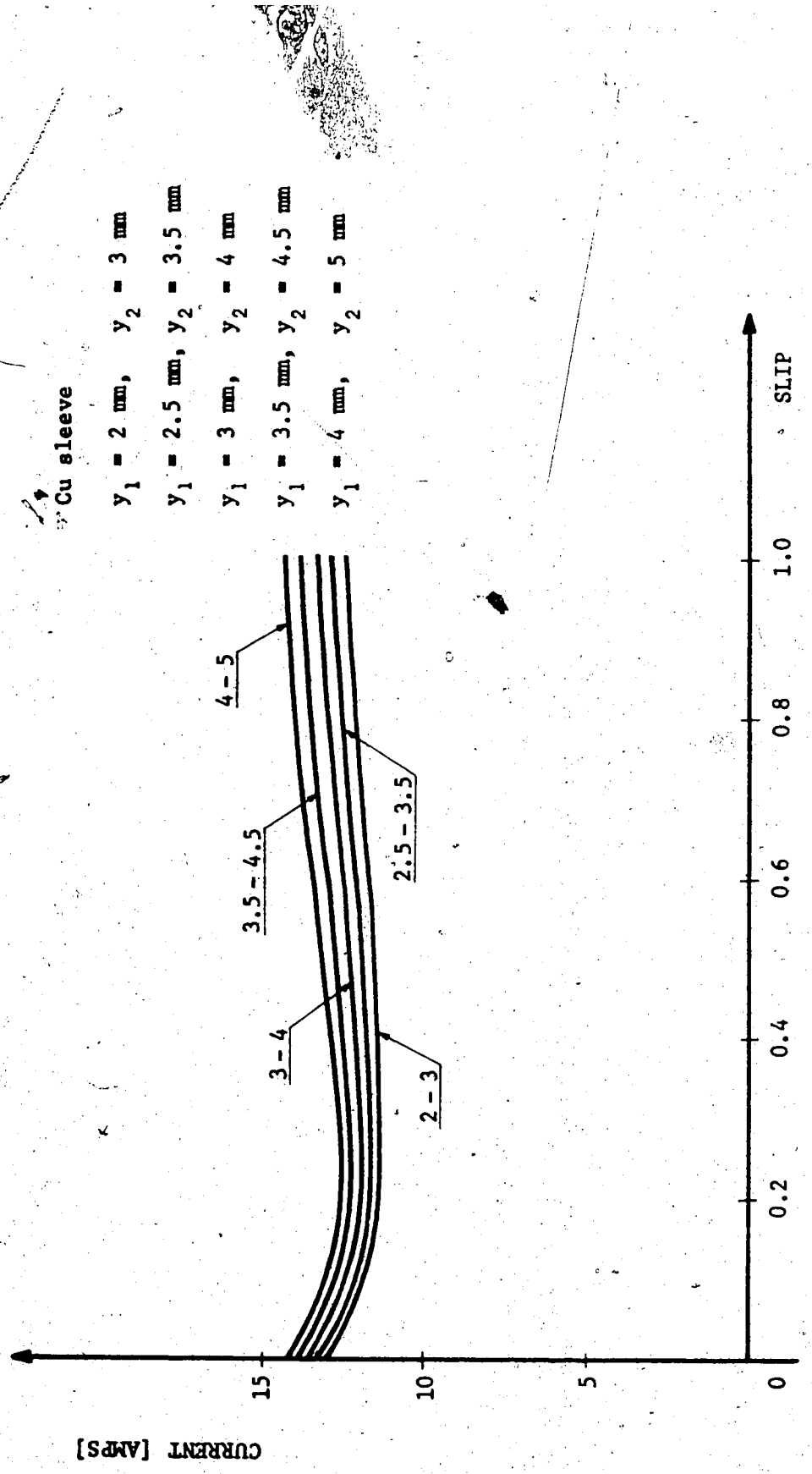

FIG. 6-23 STATOR CURRENTS

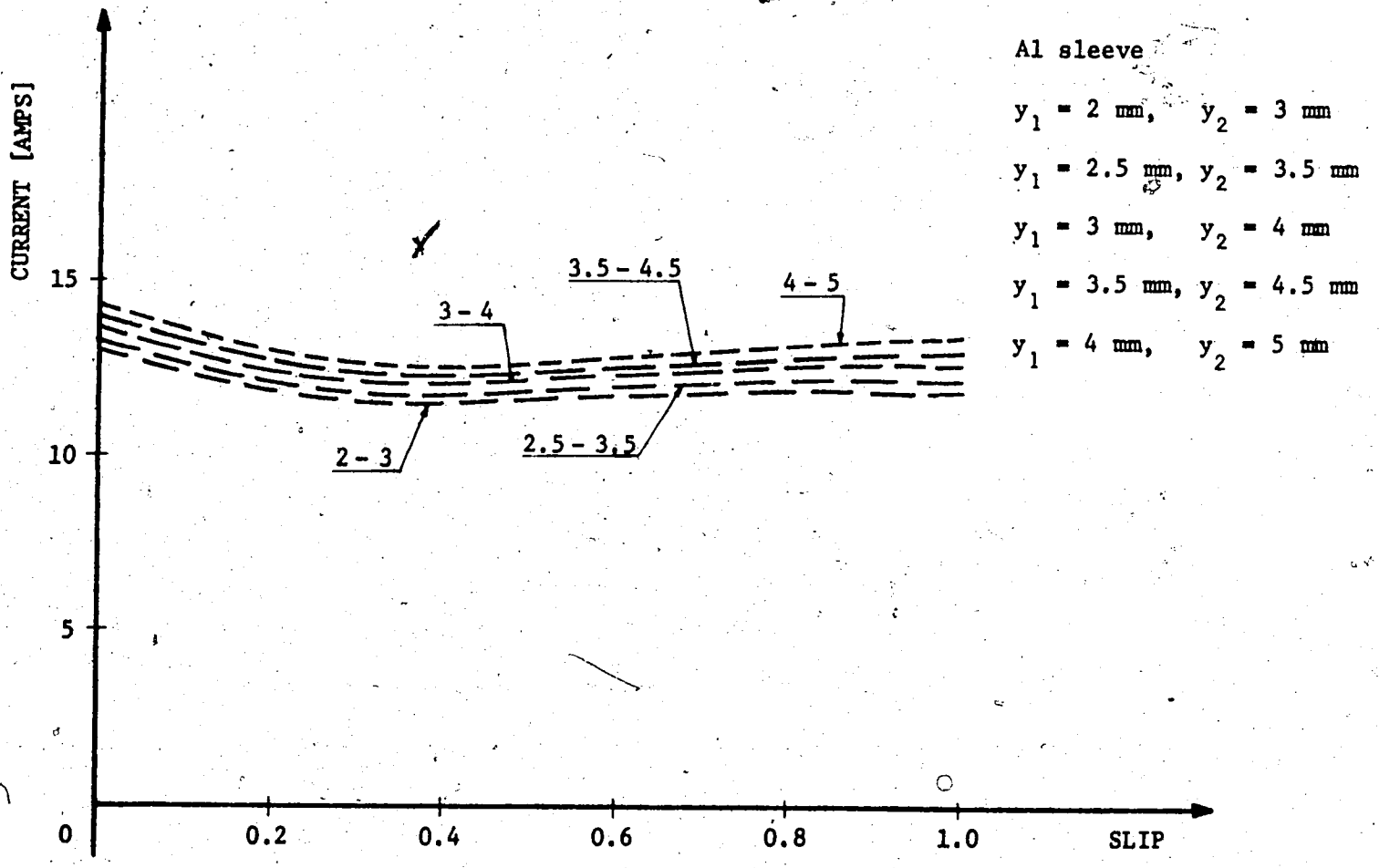

FIG. 6-24 STATOR CURRENTS

6.6. Conclusions

A tubular motor is a linear induction machine which is very simple to make. This holds especially for a machine with the type I stator winding distribution. Motors with type II and type III winding distributions are more difficult to make, but the resulting increase of efficiencies is considerable. This increase is approximately 40% for type II and 100% for type III stator windings over type I windings in our example. It is also interesting to notice the drop in the stator currents for type II and type III windings, caused by the increased inductances and rotor resistances, i.e. the total impedance of the machine is increased.

When designing a tubular motor, one should take the cost of winding and the increase of efficiencies into consideration.

Next the machine with a constant rotor sleeve thickness was considered. The air gap thickness variations showed that an increase of the air gap causes an increase of leakage inductances, thus deteriorating the machine performance. In other words, a designer of a tubular motor should keep the air gap as small as possible. The motor with fewer layers of wires in the stator winding and with the larger repeatable section τ_r would have higher efficiencies.

When the air gap thickness is kept constant and the rotor sleeve thickness is assigned different values, while the clearance is changed accordingly, the machine performance is dependent on the slip. For small slips, the increase of rotor conductivity has a bigger effect than the increase of the leakage inductances and the machine performs

better. For higher slips, however, the increased leakage inductances cause decrease of the machine performance. This means that the machine having smaller amount of rotor conductive material could perform better than a machine having a thicker rotor sleeve when the air gap thickness is concerned.

When a tubular motor has a specified clearance and a stator winding, one can change the output characteristics, using rotor with different thicknesses of the rotor sleeves. Now the air gap thickness and the rotor sleeve thickness are combined and the machine performs better for low slips, as the rotor conductor thickness is increased. For higher slips, the effect of increased leakage inductances is bigger than the effect of increased rotor conductivity and the machine performance is decreased. Therefore, when designing a tubular motor for low speeds with the clearance specified, one should design the sleeve as thin as possible. There is a limit to this, as comparison of Fig. 6-21 and Fig. 6-22 reveals that the increase of rotor resistances causes the expected decrease of the efficiencies.

The effect of higher harmonics was found negligible for the applied approximation of the hyperbolic functions for the assumed stator winding distributions. For different types of windings the approximation may not be satisfactory.

The theory used within the paper is general and may be used for LIMs. The inductance equations (3-9) hold for machines satisfying the assumptions in Chapter II.

The study presented above is applicable to the "infinitely long" tubular machines. In practice, this means that the more pole pairs the machine has, the more exact the equations are. The assumption of an infinitely long machine lies in equations (3-6). To solve the entry and exit edge effects, the different boundary conditions would have to be found; this in turn would lead to more complicated equations. It would be useful to de[illegible] the above theory by the inclusion of the edge effects, as th[illegible] performance could be predicted more exactly, especia[illegible] slips of the rotor.

REFERENCES

1. KELLY, D. H., Double Rotor Induction Motor, Ph.D. Thesis, 1968, University of Illinois

2. LAITHWAITE, E. R., Induction Machines for Special Purposes, London: Newness, 1966

3. SAUNDERS, R. M., Electromechanical Energy Conversion in Double Cylindrical Structures, A.I.E.E. Trans. Pt. 111, (Power Apparatus & Systems), Vol. 82, No. 68, Oct. 1963, pp. 631 - 638

4. NASAR, S. A., Electromagnetic Energy Conversion Devices and Systems, Prentice-Hall, 1970

5. WHITE, D. C. and WOODSON, H. H., Electromechanical Energy Conversion, John Wiley & Sons, New York, N. Y. 1959

6. MURRAY W. DAVIS, Development of Concentric Linear Induction Motor, I.E.E.E. Trans. (Power Apparatus & Systems), Vol. 91, No. 4, 1972, pp. 1506 - 1513

7. TSIH C. WANG, Linear Induction Motor for High-Speed Ground Transportation, I.E.E.E. Transactions on Industry and General Applications, Vol. IGA - 7, No. 5, Sept. 1971

8. OOI, B. T. and WHITE, D. C., Traction and Normal Forces in the Linear Induction Motor, I.E.E.E. Trans. on Power Apparatus and Systems, Vol. PAS-89, No. 4, April 1970

9. ALGER, P. L., Induction Machines, Gordon & Breach Science Publishers, New York, N. Y., 1970

10. SEELY, S., Electromechanical Energy Conversion, McGraw-Hill, 1962

11. PUCHSTEIN, A. F., LLOYD, T. C., CONRAD, A. G., Alternating Current Machines, Wiley, New York, N. Y., 1954

12. FANO, CHU, ADLER, Electromagnetic Fields Energy and Forces, Wiley, New York, N. Y., 1960

13. GUILFORD, E. C., Theory of the Induction Machine with Conducting Sleeve Rotor, A.I.E.E. Trans. Pt. 111 (Power Apparatus & Systems), Vol. 80, 1961, pp. 1129 - 1133

14. LAITHWAITE, E. R., Propulsion Without Wheels, Hart Publishing Company, New York City, 1966

15. HAGUE, B., Electromagnetic Problems in Electrical Engineering, Oxford University Press, London, 1929

16. JORDAN, E. C. and BALMAIN, K. G., Electromagnetic Waves and Radiating Systems, Prentice Hall, N. J., 1968

17. NIX, G. F., LAITHWAITE, E. R., Linear Induction Motors for Low-Speed and Standstill Application, Proc. I.E.E., Vol. 113, No. 6, June 1966

18. WOODSON, H. H., MELCHER, J. R., Electromechanical Dynamics, Wiley, New York, 1968

19. SADLER, G. V., DAVEY, A. W., Applications of Linear Induction Motors in Industry, I.E.E. Proceedings, Vol. 118, No. 6, June 1971, pp. 765 - 776

20. YAMAMURA, S., ITO, H., ISHIKAWA, Y., Theories of the Linear Induction Motor and Compensated Linear Induction Motor, I.E.E.E. Trans. Power App. & Syst., Vol. PAS - 91, No. 4, pp. 1700 - 1710, July - August 1972

APPENDIX A

Solution of Laplace's Equation

There are 3 regions to be considered for the tubular motor (Fig. 2-2):

(1) the stator conductor $y_3 \geq y \geq y_2$

(2) the air gap $y_2 \geq y \geq y_1$

(3) the rotor conductor $y_1 \geq y \geq 0$

(1) The Laplace's equation (2-24) in the air gap

$$\nabla^2 A_z = \frac{\partial^2 A}{\partial x^2} + \frac{\partial^2 A}{\partial y^2} = \sum_{\nu=1}^{\infty} \nabla^2 A_{z\nu} = 0 \qquad \nu = 1, 2, 3 \ldots . \tag{A-1}$$

has the solution of the form

$$A = A(x,y) = X(x)\, Y(y) \tag{A-2}$$

Then

$$\frac{\partial^2 A_z}{\partial x^2} = Y(y)\, X''(x)$$

$$\frac{\partial^2 A_z}{\partial y^2} = X(x)\, Y''(y)$$

and (2-24) becomes

$$Y X'' + X Y'' = 0 \tag{A-3}$$

or

$$\frac{X''}{X} = -\frac{Y''}{Y} \tag{A-4}$$

Since x and y are independent variables, they do not depend on each other and (2-24) is true only if each term in (A-4) is the same constant, therefore

$$X'' = c\,X$$

$$Y'' = -\,c\,Y$$

Let $c = -\lambda^2$, then

$$\frac{X''}{X} = \lambda^2$$

and $$\frac{Y''}{Y} = -\lambda^2$$

Therefore

$$X'' - \lambda^2 X = 0$$

and $$Y'' = -\lambda^2 Y$$

Solving the equations, we get

$$A = X(x)\,Y(y) = (B_1 \sinh\lambda y + B_2 \cosh\lambda y)\,(C \sin\lambda x + D \cos\lambda x)$$

Then

$$A_z = \mu\,[(K_1' \cosh\lambda y + K_3' \sinh\lambda y)\cos\lambda x + (K_2' \cosh\lambda y + K_4' \sinh\lambda y)\sin\lambda x] \qquad \text{(A-5)}$$

Since $$\bar{B} = \nabla \times \bar{A} = \mu\,\bar{H} = \bar{i}\,\frac{\partial A_z}{\partial y} - \bar{j}\,\frac{\partial A_z}{\partial x}$$

we have $$\mu\,H_x = \frac{\partial A_z}{\partial y}$$

and $$\mu H_y = -\frac{\partial A_z}{\partial x} = B_y \qquad \text{(A-6)}$$

Therefore, from (A-5)

$$H_x = \lambda[(K_1' \sinh\lambda y + K_3' \cosh\lambda y)\cos\lambda x + (K_2' \sinh\lambda y + K_4' \cosh\lambda y)\sin\lambda x] \qquad \text{(A-7)}$$

$$B_y = \mu\lambda[(K_1' \cosh\lambda y + K_3' \sinh\lambda y)\sin\lambda x - (K_2' \cosh\lambda y + K_4' \sinh\lambda y)\cos\lambda x] \qquad \text{(A-8)}$$

(ii) Region 1 - the stator conductor within which (2-22) holds:

$$\frac{\partial^2 A_z}{\partial x^2} + \frac{\partial^2 A_z}{\partial y^2} = -\mu(a^s \cos\lambda x^s + b^s \sin\lambda x^s)$$

and $x^s = x$, $y^s = y$, $z^s = z$, so we have

$$\frac{\partial^2 A_z}{\partial x^2} + \frac{\partial^2 A_z}{\partial y^2} = -\mu(a^s \cos\lambda x + b^s \sin\lambda x) \qquad \text{(A-9)}$$

which is satisfied by

$$A_z = \mu[(K_1 \cosh\lambda y + K_3 \sinh\lambda y)\cos\lambda x + (K_2 \cosh\lambda y + K_4 \sinh\lambda y)\sin\lambda x + \frac{1}{\lambda^2}(a^s \cos\lambda x + b^s \sin\lambda x)] \qquad \text{(A-10)}$$

Therefore

$$H_x = \lambda[(K_1 \sinh\lambda y + K_3 \cosh\lambda y)\cos\lambda x + (K_2 \sinh\lambda y + K_4 \cosh\lambda y)\sin\lambda x] \qquad \text{(A-11)}$$

$$B_y = \mu\lambda[(K_1 \cosh\lambda y + K_3 \sinh\lambda y) \sin\lambda x - (K_2 \cosh\lambda y + K_4 \sinh\lambda y) \cos\lambda x + \frac{1}{\lambda^2}(a^s \sin\lambda x - b^s \cos\lambda x)] \quad \text{(A-12)}$$

(iii) Region 3 – the rotor conductor in which (2-23) holds.

Referring the rotor currents to the stator reference frame

$$y^r = y$$

$$z^r = z$$

$$x^r = x^s - x_o{}^r = x - x_o{}^r$$

where $x_o{}^r$ is the rotor origin referred to the stator and $x_o{}^r = \dot{x}^r t$ for rotor motion gives the Galilean transformation (13, 3).

We have

$$\frac{\partial^2 A_z}{\partial x^2} + \frac{\partial^2 A_z}{\partial y^2} = -\mu(a^r \cos\lambda x^r + b^r \sin\lambda x^r) =$$

$$= -\mu[a^r \cos\lambda(x - x_o{}^r) + b^r \sin\lambda(x - x_o{}^r)] =$$

$$= -\mu\{\cos\lambda x(a^r \cos\lambda x_o{}^r - b^r \sin\lambda x_o{}^r) +$$

$$+ \sin\lambda x(a^r \sin\lambda x_o{}^r + b^r \cos\lambda x_o{}^r)]$$

The solution is of the form

$$A_z = \mu[(K_1'' \cosh\lambda y + K_3'' \sinh\lambda y) \cos\lambda x + (K_2'' \cosh\lambda y + K_4'' \sinh\lambda y) \sin\lambda x] + \frac{\mu}{\lambda^2}[(a^r \cos\lambda x_o{}^r - b^r \sin\lambda x_o{}^r) \cos\lambda x + (a^r \sin\lambda x_o{}^r + b^r \cos\lambda x_o{}^r) \sin\lambda x] \quad \text{(A-13)}$$

Therefore

$$B_y = -\lambda\mu[(K_2'' \cosh\lambda y + K_4'' \sinh\lambda y)\cos\lambda x - (K_1'' \cosh\lambda y + K_3'' \sinh\lambda y)\sin\lambda x + \frac{1}{\lambda^2}(a^r \sin\lambda x_o{}^r + b^r \cos\lambda x_o{}^r)\cos\lambda x - \frac{1}{\lambda^2}(a^r \cos\lambda x_o{}^r - b^r \sin\lambda x_o{}^r)\sin\lambda x)] \quad \text{(A-14)}$$

and

$$H_x = \lambda[(K_1'' \sinh\lambda y + K_3'' \cosh\lambda y)\cos\lambda x + (K_2'' \sinh\lambda y + K_4'' \cosh\lambda y)\sin\lambda x] \quad \text{(A-15)}$$

let

$$(a^r \sin\lambda x_o{}^r + b^r \cos\lambda x_o{}^r) = C_2$$
$$(a^r \cos\lambda x_o{}^r - b^r \sin\lambda x_o{}^r) = C_1 \quad \text{(A-16)}$$

Substituting (A-16) into (A-14)

$$B_y = \mu\lambda[(K_1'' \cosh\lambda y + K_3'' \sinh\lambda y)\sin\lambda x - (K_2'' \cosh\lambda y + K_4'' \sinh\lambda y)\cos\lambda x + \frac{1}{\lambda^2}(C_1 \sin\lambda x - C_2 \cos\lambda x)] \quad \text{(A-17)}$$

APPENDIX B

Stored Energy Calculations

(i) Evaluation of (3-2) gives

$$W_1 = \frac{\ell\mu P\pi}{4}\sum_{\nu=1}^{\infty}\nu[(K_{1\nu}^2 + K_{2\nu}^2 + K_{3\nu}^2 + K_{4\nu}^2)(\sinh\lambda_\nu y_3\cosh\lambda_\nu y_3 -$$

$$- \sinh\lambda_\nu y_2\cosh\lambda_\nu y_2) + 2(K_{1\nu}K_{3\nu} + K_{2\nu}K_{4\nu})(\sinh^2\lambda_\nu y_3 - \sinh^2\lambda_\nu y_2) +$$

$$+ \frac{2}{\lambda_\nu^2}(K_{1\nu}a^s + K_{2\nu}b^s)(\sinh\lambda_\nu y_3 - \sinh\lambda_\nu y_2) + \frac{2}{\lambda_\nu^2}(K_{3\nu}a^s +$$

$$+ K_{4\nu}b^s)(\cosh\lambda_\nu y_3 - \cosh\lambda_\nu y_2) + \frac{1}{\lambda_\nu^3}(a^{s2} + b^{s2})(y_3 - y_2)] \qquad \text{(B-1)}$$

$$W_2 = \frac{\ell\mu P\pi}{4}\sum_{\nu=1}^{\infty}\nu[(K_{1\nu}'^2 + K_{2\nu}'^2 + K_{3\nu}'^2 + K_{4\nu}'^2)(\sinh\lambda_\nu y_2\cosh\lambda_\nu y_2 -$$

$$- \sinh\lambda_\nu y_1\cosh\lambda_\nu y_1) + 2(K_{1\nu}'K_{3\nu}' + K_{2\nu}'K_{4\nu}')(\sinh^2\lambda_\nu y_2 - \sinh^2\lambda_\nu y_1)] \qquad \text{(B-2)}$$

$$W_3 = \frac{\ell\mu P\pi}{4}\sum_{\nu=1}^{\infty}\nu[(K_{1\nu}''^2 + K_{2\nu}''^2)\sinh\lambda_\nu y_1\cosh\lambda_\nu y_1 +$$

$$\frac{2}{\lambda_\nu^2}(K_1''C_1 + K_2''C_2)\sinh\lambda_\nu y_1 + \frac{y_1}{\lambda_\nu^3}(C_1^2 + C_2^2)] \qquad \text{(B-3)}$$

Because of the complexity of the above expressions, first the hyperbolic functions were represented by the first terms of the corresponding series. If the ratio of air gap thickness y_3 to

wavelength τ_r is small (17), then $\cosh\lambda y_3 \approx 1$ and $\sinh y_3 \leq 0.1$ and $\sinh\lambda y_3 \approx \lambda y_3$, $\sinh\lambda y_2 \approx \lambda y_2$, $\sinh\lambda y_1 \approx \lambda y_1$.

Also $$\sinh\lambda y_1 \leq \sinh\lambda y_2 \leq \sinh\lambda y_3$$
$$1 \leq \cosh\lambda y_1 \leq \cosh\lambda y_2 \leq \cosh\lambda y_3 \approx 1$$

Thus the set of equations (2-41) becomes

$$K_1 \approx \frac{1}{\lambda^2 y_3} (C_1 y_1 - a^s y_2)$$

$$K_2 \approx \frac{1}{\lambda^2 y_3} (C_2 y_1 - b^s y_2)$$

$$K_3 \approx \frac{1}{\lambda} (a^s y_2 - C_1 y_1)$$

$$K_4 \approx \frac{1}{\lambda} (b^s y_2 - C_2 y_1)$$

$$K_1' \approx \frac{1}{\lambda^3 y_3} [C_1 y_1 + a^s (y_3 - y_2)]$$

$$K_2' \approx \frac{1}{\lambda^3 y_3} [C_2 y_1 + b^s (y_3 - y_2)]$$

$$K_3' \approx -\frac{1}{\lambda} C_1 y_1$$

$$K_4' \approx -\frac{1}{\lambda} C_2 y_1$$

$$K_1'' \approx \frac{1}{\lambda^2 y_3} [a^s(y_3 - y_2) - C_1(y_3 - y_1)]$$

$$K_2'' \approx \frac{1}{\lambda^2 y_3} [b^s(y_3 - y_2) - C_2(y_3 - y_1)] \qquad \text{(B-4)}$$

Substituting (B-4) into (B-1) to (B-3), we have

$$W_1 = \frac{\ell\mu P\pi}{4} \sum_{\nu=1}^{\infty} \frac{\nu}{\lambda_\nu^3 y_3} \left\{ \left[a^{s2} + b^{s2} \right] \left[\frac{y_2^2 (y_3 - y_2)}{y_3} - 2\, y_2 (y_3 - y_2) + \right.\right.$$

$$\left. + y_3 (y_3 - y_2) + \lambda_\nu^2\, y_2^2\, y_3 (y_3 - y_2) - 2\, \lambda_\nu^2\, y_2^2 (y_3^2 - y_2^2) \right] +$$

$$+ \left[C_1^2 + C_2^2 \right] \left[\frac{y_1^2 (y_3 - y_2)}{y_3} + \lambda_\nu^2\, y_1^2\, y_3 (y_3 - y_2) - 2\, \lambda_\nu^2\, y_1^2 (y_3^2 - y_2^2) \right] +$$

$$+ 2 \left[C_1\, a^s + C_2\, b^s \right] \left[y_1 (y_3 - y_2) - \frac{y_1 y_2 (y_3 - y_2)}{y_3} + 2\, \lambda_\nu^2\, y_1 y_2 (y_3^2 - y_2^2) - \right.$$

$$\left.\left. - \lambda_\nu^2\, y_1 y_2 y_3 (y_3 - y_2) \right] \right\} \qquad \text{(B-5)}$$

$$W_2 = \frac{\ell\mu P\pi}{4} \sum_{\nu=1}^{\infty} \frac{\nu}{\lambda_\nu^3 y_3} \left\{ \left[a^{s2} + b^{s2} \right] \left[\frac{(y_2 - y_1)(y_3 - y_2)^2}{y_3} \right] + \right.$$

$$+ \left[C_1^2 + C_2^2 \right] \left[\frac{y_1^2 (y_2 - y_1)}{y_3} - 2\, \lambda_\nu^2 (y_2^2 - y_1^2)\, y_1^2 + \lambda_\nu^2\, y_1^2\, y_3 (y_2 - y_1) \right] +$$

$$\left. + 2 \left[C_1\, a^s + C_2\, b^s \right] \left[\frac{y_1}{y_3} (y_3 - y_2)(y_2 - y_1) - \lambda_\nu^2\, y_1 (y_3 - y_2)(y_2^2 - y_1^2) \right] \right\}$$

$$\text{(B-6)}$$

$$W_3 = \frac{\ell\mu P\pi}{4} \sum_{\nu=1}^{\infty} \frac{\nu}{\lambda_\nu^3 y_3} \left\{ \left[a^{s2} + b^{s2} \right] \left[\frac{y_1}{y_3} (y_3 - y_2)^2 \right] + \right.$$

$$+ \left[C_1^2 + C_2^2 \right] \left[\frac{y_1}{y_3} (y_3 - y_1)^2 - 2\, y_1 (y_3 - y_1) + y_1\, y_3 \right] +$$

$$\left. + 2 \left[C_1\, a^s + C_2\, b^s \right] \left[y_1 (y_3 - y_2) - \frac{y_1}{y_3} (y_3 - y_2)(y_3 - y_1) \right] \right\} \qquad \text{(B-7)}$$

Inductances of the equivalent machine were determined from the above equations as

$$L_{ss\nu} = \frac{P\ell\mu\tau (K_{a\nu}{}^s)^2}{4\, \lambda_\nu\, y_3} \left[1 - \lambda_\nu^2\, y_2^2\, \frac{2\, y_2 + y_3}{y_3 - y_2} \right]$$

$$L_{rr\nu} = \frac{P\ell\mu\tau (K_{a\nu}{}^s)^2}{4\, \lambda_\nu\, y_3} \left[1 + \lambda_\nu^2\, (2\, y_1^2 - y_1\, y_2 - y_3^2) \right]$$

$$L_{sr\nu} = \frac{P\ell\mu\tau (K_{a\nu}{}^s)^2}{4\, \lambda_\nu\, y_3} \left[1 + \lambda_\nu^2\, (y_1^2 + y_2^2 + y_2\, y_3) \right] \qquad \text{(B-8)}$$

resulting in $L_{sr\nu} > L_{ss\nu} > L_{rr\nu}$ and negative leakage inductances of both the rotor and stator. Therefore the above approach was not used.

(ii) Instead, equations (2-40) were substituted into (B-1) to (B-3), resulting in the following:

$$W_1 = (\ell\mu P\pi)/4 \sum_{\nu=1}^{\infty} \nu \{[(C_1^2 + C_2^2)/\lambda^4]\ [(\sinh^2\lambda y_1 \coth^2\lambda y_3 +$$

$$+ \sinh^2\lambda y_1)\ (\sinh\lambda y_3 \cosh\lambda y_3 - \sinh\lambda y_2 \cosh\lambda y_2) -$$

$$- 2 \sinh^2\lambda y_1 \coth\lambda y_3\ (\sinh^2\lambda y_3 - \sinh^2\lambda y_2)] +$$

$$+ [(a^{s2} + b^{s2})/\lambda^4]\ [(\sinh^2\lambda y_2 \coth^2\lambda y_3 +$$

$$+ \sinh^2\lambda y_2)\ (\sinh\lambda y_3 \cosh\lambda y_3 - \sinh\lambda y_2 \cosh\lambda y_2) -$$

$$- 2 \sinh^2\lambda y_2 \coth\lambda y_3\ (\sinh^2\lambda y_3 - \sinh^2\lambda y_2) -$$

$$- 2 \sinh\lambda y_2 \coth\lambda y_3\ (\sinh\lambda y_3 - \sinh\lambda y_2) +$$

$$+ 2 \sinh\lambda y_2\ (\cosh\lambda y_3 - \cosh\lambda y_2) + \lambda(y_3 - y_2)] +$$

$$+ [(2C_1 a^s + 2C_2 b^s)/\lambda^4]\ [\sinh\lambda y_1 \coth\lambda y_3\ (\sinh\lambda y_3 - \sinh\lambda y_2) -$$

$$- (\sinh\lambda y_1 \sinh\lambda y_2 \coth^2\lambda y_3 + \sinh\lambda y_1 \sinh\lambda y_2)(\sinh\lambda y_3 \cosh\lambda y_3 -$$

$$- \sinh\lambda y_2 \cosh\lambda y_2) - \sinh\lambda y_1\ (\cosh\lambda y_3 - \cosh\lambda y_2) +$$

$$+ 2 \sinh\lambda y_1 \sinh\lambda y_2 \coth\lambda y_3\ (\sinh^2\lambda y_3 - \sinh^2\lambda y_2)]\}$$

(B-9)

$$W_2 = (\ell\mu P\pi)/4 \sum_{\nu=1}^{\infty} \nu \{[(C_1^2 + C_2^2)/\lambda^4] [(\sinh^2\lambda y_1 \coth^2\lambda y_3 +$$

$$+ \sinh^2\lambda y_1) (\sinh\lambda y_2 \cosh\lambda y_2 - \sinh\lambda y_1 \cosh\lambda y_1) -$$

$$- 2 \sinh^2\lambda y_1 \coth\lambda y_3 (\sinh^2\lambda y_2 - \sinh^2\lambda y_1)] +$$

$$+ [(a^{s2} + b^{s2})/\lambda 4] [(\sinh^2\lambda y_2 \coth^2\lambda y_3 + \cosh^2\lambda y_2 -$$

$$- 2 \sinh\lambda y_2 \cosh\lambda y_2 \coth\lambda y_3) (\sinh\lambda y_2 \cosh\lambda y_2 -$$

$$- \sinh\lambda y_1 \cosh\lambda y_1)] +$$

$$+ [2 (C_1 a^s + C_2 b^s)/\lambda^4] [(\sinh\lambda y_1 \cosh\lambda y_2 \coth\lambda y_3 -$$

$$- \sinh\lambda y_1 \sinh\lambda y_2 \coth^2\lambda y_3) (\sinh\lambda y_2 \cosh\lambda y_2 -$$

$$- \sinh\lambda y_1 \cosh\lambda y_1) + (\sinh\lambda y_1 \sinh\lambda y_2 \coth\lambda y_3 -$$

$$- \sinh\lambda y_1 \cosh\lambda y_2) (\sinh^2\lambda y_2 - \sinh^2\lambda y_1)]\} \qquad \text{(B-10)}$$

$$W_3 = (\ell\mu P\pi)/4 \sum_{\nu=1}^{\infty} \nu \{[(C_1^2 + C_2^2)/\lambda^4] [2 \sinh\lambda y_1 (\sinh\lambda y_1 \coth\lambda y_3 -$$

$$- \cosh\lambda y_1) + \lambda y_1 + (\sinh^2\lambda y_1 \coth^2\lambda y_3 + \cosh^2\lambda y_1 -$$

$$- 2 \sinh\lambda y_1 \cosh\lambda y_1 \coth\lambda y_3) \sinh\lambda y_1 \cosh\lambda y_1] +$$

$$+ [(a^{s2} + b^{s2})/\lambda^4] [(\sinh^2\lambda y_2 \coth^2\lambda y_3 + \cosh^2\lambda y_2 -$$

$$- 2 \sinh\lambda y_2 \cosh\lambda y_2 \coth\lambda y_3) \sinh\lambda y_1 \cosh\lambda y_1] +$$

$$+ [2 (C_1 a^s + C_2 b^s)/\lambda^4] [(\sinh\lambda y_1 \cosh\lambda y_2 \coth\lambda y_3 -$$

$$- \sinh\lambda y_1 \sinh\lambda y_2 \coth^2\lambda y_3 - \cosh\lambda y_1 \cosh\lambda y_2 +$$

$$+ \cosh\lambda y_1 \sinh\lambda y_2 \coth\lambda y_3) \sinh\lambda y_1 \cosh\lambda y_1 +$$

$$+ (\cosh\lambda y_2 - \sinh\lambda y_2 \coth\lambda y_3) \sinh\lambda y_1]\} \qquad \text{(B-11)}$$

APPENDIX C

MACHINE DATA AND CALCULATIONS

C-1 Machine Data

The machine can employ different rotors, as they are easy to replace. This is a big advantage of tubular motors, as different characteristics of the machine can be obtained simply by inserting rotors with different thickness of the conducting sleeve and/or different sleeve material.

The idealized machine used for digital analysis has the following data:

Overall diameter of machine	7 cm
Thickness of stator winding	0.6005 cm
Stator length	24.2 cm
Power supply	110 V, two phase, 60 Hz
Stator winding	432 turns per τ_r per phase
Wire	#18, 7.76 Ω per 1000' at 75°C
Rotor sleeve	copper, $\sigma = 4.93 \times 10^7$ mhos/metre at 75°C
	aluminum, $\sigma = 2.97 \times 10^7$ mhos/metre at 75°C
Four pole stator	$\tau_r = 12.1$ cm, $v^s = \tau_r f = 7.26$ m/sec.

C-2 Stator Windings

A simple stator winding such as one having the current density distribution shown in Fig. 2-3 will be called type I stator winding. The distribution factors are derived from (2-3), giving

$$K^s_{a\nu} = \frac{8N}{\tau_r} \frac{\sin\frac{\pi\nu}{4}}{\frac{\pi\nu}{2}} \cos\frac{\pi\nu}{4} \qquad \text{(C-1)}$$

where N is the number of conductors within the shaded area in Fig. 2-3.

We have

$$K^s_{a\nu} = K^s_{b\nu}$$

due to the symmetry of the windings.

Type II stator winding has the stator current density distribution as shown in Fig. 2-5. From equation (2-3) we have

$$K^s_{a\nu} = \frac{2N}{\tau_r} \frac{\sin\frac{\pi\nu}{8}}{\frac{\pi\nu}{8}} \left[2\cos(\nu 0) + \cos\frac{\pi\nu}{4} - \right.$$

$$\left. - \cos\frac{3\pi\nu}{4} - 2\cos\pi\nu - \cos\frac{5\pi\nu}{4} + \cos\frac{7\pi\nu}{4}\right] \qquad \text{(C-2)}$$

where N is the number of conductors within the shaded area in Fig. 2-5.

Winding is symmetric, therefore

$$K^s_{a\nu} = K^s_{b\nu}$$

Type III stator windings have current density distributions shown in Fig. 2-6. Substituting into (2-3)

$$K^s_{a\nu} = \frac{4N}{\tau_r} \frac{\sin \frac{\pi\nu}{12}}{\frac{\pi\nu}{12}} \left[3 + 2 \cos \frac{\pi\nu}{6} + \cos \frac{\pi\nu}{3} - \right.$$

$$\left. - \cos \frac{2\pi\nu}{3} - 2 \cos \frac{5\pi\nu}{6}\right] \qquad \text{(C-3)}$$

where N is the number of conductors within the shaded area in Fig. 2-6.

We have again

$$K^s_{a\nu} = K^s_{b\nu}$$

The winding distribution factors for three types of stator winding distributions are listed in Table 1. The amplitude of the first harmonic is the largest and the machine will run on this predominant harmonic.

ν	$K_{av\nu}$ [turns/metre]		
	Type I	Type II	Type III
1	4546	5939	8572
3	- 1515	820.1	714.3
5	909.2	492	- 1714
7	- 649.4	848.5	- 1225
9	505.1	- 659.9	238.1
11	- 413.3	- 223.7	779.2

TABLE 1 WINDING DISTRIBUTION FACTORS

C-3 Digital Programs

The program in Table 2 is written for inductances derived from equation (3-3) for magnetic stored energy. The hyperbolic functions are preserved and therefore even higher harmonic inductances are exact (for the assumptions in Chapter II).

Table 3 lists the program based on the equation (3-4) for the inductances where approximations were used. They introduce an error into the higher harmonic inductances.

Both programs in Table 2 and Table 3 are used for the type I winding distribution. The calculations of type II and type III winding distribution machines were done with the programs in Table 4 and Table 5 respectively, in which approximations of hyperbolic functions were used.

```
      ∇F[□]∇
    ∇ PH←F S
[1]   B←ρA
[2]   G←2×P×A+TR
[3]   C←ρS
[4]   KAN←16×N×(10P×A+4)×(20P×A+4)+TR×P×A
[5]   R75←PP×R75
[6]   MM←(C,B)ρMM←PP×Z×(TR*3)×(KAN*2)×M+16×Y3×(P×A)*2
[7]   LSS←MM×LSS←(C,B)ρ(((((50G×Y2)×(((50G×Y2)×(60G×Y3)+50G×Y3)-60G×Y2))+G×Y3-Y2)×Y3+(Y3-
      Y2)*2)+G
[8]   LRR←MM×LRR←(C,B)ρ((((((50G×Y1)*2)×(60G×Y3)+(50G×Y3))-((50G×Y1)×(60G×Y1)))+Y1×G)×Y3
      +Y1*2)+G
[9]   LSR←MM×LSR←(C,B)ρ((((50G×Y1)×(60G×Y2))-(50G×Y1)×(50G×Y2)×(60G×Y3)+50G×Y3)×Y3+Y1×Y3
      -Y2)+G
[10]  SN←Q(B,C)ρS,(4-3×S),(¯4+5×S),(8-7×S),(¯8+9×S),(12-11×S)
[11]  RR←(C,B)ρ((KAN*2)×PP×TR×Z+4×CR75×Y1)
[12]  CQ←(SN×(W×LSR)*2)+(RR*2)+(SN×W×LRR)*2
[13]  ZSQ←Q(B,C)ρZSQ1←ZSQ1←((R75+(+/RR×CQ))*2)+((+/W×LSS)-(+/W×CQ×LRR×SN))*2
[14]  A←(C,B)ρA
[15]  POR←+/PH←((C,B)ρ(×KAN))×RR×CQ×4×A×P×(V*2)+TR×W×ZSQ
[16]  SL←R75×ISQ←(V*2)+ZSQ1
[17]  RL←+/((C,B)ρ(RR×SN×CQ×(V*2)+ZSQ))
[18]  RO←+/((C,B)ρ(×KAN))×((RR+SN)-RR)×SN×CQ×(V*2)+ZSQ
[19]  PN←EF←100×PO+RO+SL+RL
      ∇
```

TABLE 2 DIGITAL PROGRAM - TYPE I WINDING
(inductances not simplified)

```
      ∇F[⎕]∇
    ∇ FN←F S
[1]   B←⍴A
[2]   C←⍴S
[3]   KAN←16×N×(10P×A+4)×(20P×A+4)+TR×P×A
[4]   R75←PP×R75
[5]   MM←(C,B)⍴MM←PP×Z×(TR*3)×(KAN*2)×M+16×Y3×(P×A)*2
[6]   LSS←MM×LSS←(C,B)⍴(1+((2×P×A×Y2+TR)*2)+3)
[7]   LRR←MM×LRR←(C,B)⍴(1+((2×P×A×(Y3-Y1)+TR)*2)+3)
[8]   LSR←MM×LSR←(C,B)⍴(1+((2×P×A+TR)*2)×((Y1*2)+(Y2*2)-2×Y2×Y3)+6)
[9]   SN←⍉(B,C)⍴S,(4-3×S),(¯4+5×S),(8-7×S),(¯8+9×S),(12-11×S)
[10]  RR←(C,B)⍴((KAN*2)×PP×TR×Z+4×CR75×Y1)
[11]  CQ←(SN×(W×LSR)*2)+(RR*2)+(SN×W×LRR)*2
[12]  ZSQ←⍉(B,C)⍴ZSQ1←ZSQ1←((R75+(+/RR×CQ))*2)+((+/W×LSS)-(+/W×CQ×LRR×SN))*2
[13]  A←(C,B)⍴A
[14]  FOR←+/FH←((C,B)⍴(×KAN))×RR×CQ×4×A×P×(V*2)+TR×W×ZSQ
[15]  SL←R75×ISQ←(V*2)+ZSQ1
[16]  RL←+/((C,B)⍴(RR×SN×CQ×(V*2)+ZSQ))
[17]  RO←+/((C,B)⍴(×KAN))×((RR+SN)-RR)×SN×CQ×(V*2)+ZSQ
[18]  FN←EF←100×RO+RO+SL+RL
      ∇
```

TABLE 3 DIGITAL PROGRAM - TYPE I WINDING

```
      ∇F[□]∇
    ∇ FN←F S
[1]   B←ρA
[2]   C←ρS
[3]   KAN←64×N×(10P×A÷8)×(1+(20P×A÷4))÷TR×P×A
[4]   R75←PP×R75
[5]   MM←(C,B)ρMM←PP×Z×(TR*3)×(KAN*2)×M÷16×Y3×(P×A)*2
[6]   LSS←MM×LSS←(C,B)ρ(1+((2×P×A×Y2÷TR)*2)÷3)
[7]   LRR←MM×LRR←(C,B)ρ(1+((2×P×A×(Y3-Y1)÷TR)*2)÷3)
[8]   LSR←MM×LSR←(C,B)ρ(1+((2×P×A÷TR)*2)×((Y1*2)+(Y2*2)-2×Y2×Y3)÷6)
[9]   SN←⍉(B,C)ρS,(¯2+3×S),(¯4+5×S),(¯6+7×S),(10-9×S),(12-11×S)
[10]  RR←(C,B)ρ((KAN*2)×PP×TR×Z÷4×CR75×Y1)
[11]  CQ←(SN×(W×LSR)*2)÷(RR*2)+(SN×W×LRR)*2
[12]  ZSQ←⍉(B,C)ρZSQ1←ZSQ1←((R75+(+/RR×CQ))*2)+((+/W×LSS)-(+/W×CQ×LRR×SN))*2
[13]  A←(C,B)ρA
[14]  FOR←+/FH←((C,B)ρ(×KAN))×RR×CQ×4×A×P×(V*2)÷TR×W×ZSQ
[15]  SL←R75×ISQ←(V*2)÷ZSQ1
[16]  RL←+/((C,B)ρ(RR×SN×CQ×(V*2)÷ZSQ))
[17]  RO←+/((C,B)ρ(×KAN))×((RR÷SN)-RR)×SN×CQ×(V*2)÷ZSQ
[18]  FN←EF←100×RO÷RO+SL+RL
    ∇
```

TABLE 4 DIGITAL PROGRAM - TYPE II WINDING

```
      ∇F[⎕]∇
    ∇ FN←F S
[1]   B←⍴A
[2]   C←⍴S
[3]   KAN←96×N×(10P×A÷12)×(1.5+(20P×A÷3)+(4×(20P×A÷6)))÷TR×P×A
[4]   R75←PP×R75
[5]   MM←(C,B)⍴MM←PP×Z×(TR*3)×(KAN*2)×[illegible]÷16×Y3×(P×A)*2
[6]   LSS←MM×LSS←(C,B)⍴(1+((2×P×A×Y2÷TR)*2)÷3)
[7]   LRR←MM×LRR←(C,B)⍴(1+((2×P×A×(Y3-Y1)÷TR)*2)÷3)
[8]   LSR←MM×LSR←(C,B)⍴(1+((2×P×A÷TR)*2)×((Y1*2)+(Y2*2)-2×Y2×Y3)÷6)
[9]   SN←⍉(B,C)⍴S,(¯2+3×S),(¯4+5×S),(¯6+7×S),(¯8+9×S),(¯10+11×S)
[10]  RR←(C,B)⍴((KAN*2)×PP×TR×Z÷4×CR75×Y1)
[11]  CQ←(SN×(W×LSR)*2)  [illegible]R*2)+(SN×W×LRR)*2
[12]  ZSQ←⍉(B,C)⍴ZSQ1←Z  1←((R75+(+/RR×CQ))*2)+((+/W×LSS)-(+/W×CQ×LRR×SN))*2
[13]  A←(C,B)⍴A
[14]  FOR←+/FH←((C,B)⍴(×KAN))×RR×CQ×4×A×P×(V*2)÷TR×W×ZSQ
[15]  SL←R75×ISQ←(V*2)÷ZSQ1
[16]  RL←+/((C,B)⍴(RR×SN×CQ×(V*2)÷ZSQ))
[17]  RO←+/(((C,B)⍴(×KAN))×((RR÷SN)-RR)×SN×CQ×(V*2)÷ZSQ
[18]  FN←EF←100×RO÷RO+SL+RL
    ∇
```

TABLE 5 DIGITAL PROGRAM - TYPE III WINDING

C-4 Inductances

A comparison between the two programs showed, as expected, an increase of the error as the air gap was increased. For large air gaps (i.e. $y_1 = 0.25$ cm, $y_2 = 0.5$ cm), the error for the first harmonic inductances was less than 0.2%, while for the third harmonic it was almost 10%. The overall effect on the machine performance was negligible, the only considerable error being for zero slip as the effect of higher harmonics was stressed.

For machines having very large air gaps or having stator winding distribution with considerable higher harmonics or for machines running on the higher harmonic, the program with hyperbolic functions must be used.

As the values of the air gap and rotor sleeve were changed, the machine parameters changed too, therefore, next is an example of parameters for $y_1 = 0.2$ cm and $y_2 = 0.3$ cm only. The machine has a type I winding.

ν	1	3	5	7	9	11
$R^r_{a\nu}$ [ohms]	2.43	0.27	0.09719	0.04958	0.03	0.02008

TABLE 6 ROTOR RESISTANCES

ν	Program in Table 1			Program in Table 2		
	$L_{ss\nu}$	$L_{sr\nu}$	$L_{rr\nu}$	$L_{ss\nu}$	$L_{sr\nu}$	$L_{rr\nu}$
1	12500	12170	12940	12500	12170	12950
3	162.5	131.6	204.8	164.2	127.7	213.8
5	22.48	13.77	34.71	23.85	10.69	41.71
7	6.188	2.806	11.05	7.211	0.499	16.32
9	2.361	0.8007	4.663	3.128	- 9.932	8.64
11	1.091	- 0.2817	2.314	1.676	- 1.042	5.366

TABLE 7 INDUCTANCES [μH]